PASSIVE VISCOELASTIC CONSTRAINED LAYER DAMPING FOR STRUCTURAL APPLICATION

A THESIS SUBMITTED IN PARTIAL FULFILLMENT OF
THE REQUIREMENTS FOR THE DEGREE OF

MASTER OF TECHNOLOGY
IN
MECHANICAL ENGINEERING

[Specialization: Machine Design and Analysis]

By

PALASH DEWANGAN

207ME109

Department of Mechanical Engineering

NATIONAL INSTITUTE OF TECHNOLOGY
ROURKELA

MAY, 2009

PASSIVE VISCOELASTIC CONSTRAINED LAYER DAMPING FOR STRUCTURAL APPLICATION

A THESIS SUBMITTED IN PARTIAL FULFILLMENT OF
THE REQUIREMENTS FOR THE DEGREE OF

MASTER OF TECHNOLOGY
IN
MECHANICAL ENGINEERING

[Specialization: Machine Design and Analysis]

By

PALASH DEWANGAN

207ME109

Under the supervision of

Prof. B.K.NANDA
NIT Rourkela

Department of Mechanical Engineering

NATIONAL INSTITUTE OF TECHNOLOGY
ROURKELA

MAY, 2009

Dedicated to my parents

*

National Institute of Technology

Rourkela

CERTIFICATE

This is to certify that the work in this project report entitled **Passive Viscoelastic Constrained Layer Damping For Structural Application** by **Palash Dewangan** has been carried out under our supervision in partial fulfillment of the requirements for the degree of **Master of Technology** in *Mechanical Engineering* with ***Machine Design and Analysis*** specialization during session 2008 - 2009 in the Department of Mechanical Engineering, National Institute of Technology, Rourkela.

To the best of our knowledge, this work has not been submitted to any other University/Institute for the award of any degree or diploma.

(supervisor)

Dr. B.K.Nanda

Professor

Dept. of Mechanical Engineering

National Institute of Technology, Rourkela

ACKNOWLEDGEMENT

Setting an endeavour may not always be an easy task, obstacles are bound to come in this way & when this happens, help is welcome & needless to say without help of the those people whom I am going to address here, this endeavour could not have been successful & I owe my deep sense of gratitude & warm regards to my supervisor **Dr.B. K. Nanda, Dept of Mechanical Engineering, NIT Rourkela** for suggesting me an exhaustive & challenging topic pertaining to my dissertation work as well as his able monitoring throughout the course of my work. I am greatly indebted to him for his constructive suggestions.

I extend my thanks to **Dr. R. K. Sahoo, Professor and Head, Dept. of Mechanical Engineering** for extending all possible help in carrying out the dissertation work directly or indirectly.

I further cordially present my gratitude to **Mr.H.Roy** for his indebted help and valuable suggestion for accomplishment of my dissertation work.

I greatly appreciate & convey my heartfelt thanks to my colleagues' flow of ideas, dear ones & all those who helped me in completion of this work.

Special thanks to my parents & elders without their blessings & moral enrichment I could not have landed with this outcome.

Above all, even though, he does not need any credit, but my prayers & ovations to the Omnipotent**,** who strengthened me to stand with smile against the odds coming in this course of work without fail & blessed me with this fruit of work for my dedication.

PALASH DEWANGAN

ABSTRACT

The purpose behind this study is to predict damping effects using method of passive viscoelastic constrained layer damping. Ross, Kerwin and Unger (RKU) model for passive viscoelastic damping has been used to predict damping effects in constrained layer sandwich cantilever beam. This method of passive damping treatment is widely used for structural application in many industries like automobile, aerospace, etc.

The RKU method has been applied to a cantilever beam because beam is a major part of a structure and this prediction may further leads to utilize for different kinds of structural application according to design requirements in many industries. In this method of damping a simple cantilever beam is treated by making sandwich structure to make the beam damp, and this is usually done by using viscoelastic material as a core to ensure the damping effect. Since few years in past viscoelastic materials has been significantly recognized as the best damping material for damping application which are usually polymers. Here some viscoelastic materials have been used as a core for sandwich beam to ensure damping effect.

Due to inherent complex properties of viscoelastic materials, its modeling has been the matter of talk. So in this report modeling of viscoelastic materials has been shown and damping treatment has been carried out using RKU model. The experimental results have been shown how the amplitude decreases with time for damped system compared to undamped system and further its prediction has been extended to finite element analysis with various damping material to show comparison of harmonic responses between damped and undamped systems.

Contents

List of figures

List of Tables

Chapter 1

Introduction

1.1 Vibration problem and evolution of passive damping technology

The damping of structural components and materials is often a significantly overlooked criterion for good mechanical design. The lack of damping in structural components has led to numerous mechanical failures over a seemingly infinite multitude of structures. For accounting the damping effects, lots of research and efforts have been done in this field to suppress vibration and to reduce the mechanical failures.

Since it was discovered that damping materials could be used as treatments in passive damping technology to structures to improve damping performance, there has been a flurry of ongoing research over the last few decades to either alter existing materials, or develop entirely new materials to improve the structural dynamics of components to which a damping material could be applied. The most common damping materials available on the current market are viscoelastic materials. Viscoelastic materials are generally polymers, which allow a wide range of different compositions resulting in different material properties and behavior. Thus, viscoelastic damping materials can be developed and tailored fairly efficiently for a specific application.

1.2 Finite Element Analysis for thin damped sandwich beams

Finite element analysis has emerged as a very efficient tool for solving complex problem in field of design engineering. The experimental procedure is a very tedious task and lots of assumption must be taken care off for precision of the work and using finite element method we can reduce this complexity of the problem and get rid of calculations. In this report a finite element analysis has been done for both undamped and damped sandwich structures and frequency response for the same has been shown.

1.3 Objective of the present work

This report provides a final summary of the progress made over the past year on the study of passive viscoelastic constrained layer damping, specifically applied to high stiffness structural members. Viscoelastic materials are materials which dissipate system energy when deformed in shear. This damping technology has a wide variety of engineering applications, including bridges, engine mounts, and machine components such as rotating shafts, component vibration isolation, novel spring designs which incorporate damping without the use of traditional dashpots or shock absorbers, and structural supports.

The main focus of this dissertation is to study the complex behavior of the viscoelastic materials, to predict damping effects using method of passive viscoelastic constrained layer damping technology experimentally and to show the nature of response of structures using finite element method.

Chapter 2
Literature Review

2.1 Introduction

Noise and vibration control [1] is a major concern in several industries such as aeronautics and automobiles. The reduction of noise and vibrations is a major requirement for performance, sound quality, and customer satisfaction. Passive damping technology [2, 3] using viscoelastic materials are classically used to control vibration. The steel industry proposes damped sandwich sheets in which a thin layer of viscoelastic material is sandwiched between two elastic face layers.

The growing use of such structures has motivated many authors to intensify the study of their vibration and acoustic performance and the design of sandwich damped structures. This kind of structures has appeared recently as a viable alternative. It has been shown that this class of materials enables manufacturers to cut weight and cost while providing noise, vibration and harshness performance. Although initially confined to the aerospace field, laminated structures with a viscoelastic core are now applied in almost all industrial fields.

2.2Constrained Layer Viscoelastic Damping (Damped Sandwich Structure)

The fundamental work in this field was pioneered by Ross, Kerwin and Ungar (RKU) [5], who used a three-layer model to predict damping in plates with constrained layer damping treatments. Kerwin [6] was the first to present a theoretical approach of damped thin structures with a constrained viscoelastic layer. He stated that the energy dissipation mechanism in the constrained core is attributable to its shear motion. He presented the first analysis of the simply supported sandwich beam using a complex modulus to represent the viscoelastic core. Several authors DiTaranto [7], Mead and Markus [8] extended Kerwin's work using his same basic assumptions. DiTaranto proposed an exact sixth-order theory for the unsymmetrical three-layer beam, and this was subsequently refined [8-10].

A fourth-order equation of motion was developed by Yan and Dowell [11], for beams and plates. Shear motion in the faces and rotational inertia are taken into account to obtain a sixth-order equation, which is simplified to the fourth order. In 1982, Mead [12], reviewed previous theories and stated that most authors made the same basic assumptions and concluded that all the theories must predict the same loss factors. This set of assumptions is known in the literature by "Mead and Markus model" [8]. Yu [13] included in its study the effects of the rotational inertia and longitudinal displacement for the symmetrical plates. Rao and Nakra [14, 15] included these same effects in their equation of motion of unsymmetrical plates and beams. Most of the authors cited above have neglected the effect of shearing in the skins. Durocher and Solecki [16] included the shearing effects in the skins in the symmetrical plate model and ensured the continuity of displacements and shear stresses at the interfaces. In Ref. [12], the simplified model of Yan and Dowell as well as the models of DiTaranto and Mead and Markus are validated and compared with an accurate differential equation accounting for shearing and rotational inertia in the skins as well as the discrete displacement field of the layers.

An analytical method considering flexural, longitudinal, rotational, and shear deformations in all layers of sandwich beams with multiple constrained layer damping patches is proposed by Kung [17]. The method is verified by comparing results for a single patch with those reported in the literature by Lall [18] and Rao[10] . Two wave-based approaches are proposed by Ghinet and Atalla [19]. The first concerns the modeling of a thick flat sandwich composite; it uses a discrete displacement field for each layer and allows for out of plane displacements and shearing rotations. Good results were obtained compared to experimental data. The second concerns the modeling of thick laminate structures. Each layer is described by a Reissner–Mindlin displacement field, and equilibrium relations account for membrane, transversal shearing, bending, and full inertial terms. The discrete displacement of each layer leads to accuracy over a wide frequency range. The model is successfully validated with numerical classical spectral finite elements and experimental results.

2.3 The Finite Element Method

In practice it is often necessary to design damped structures with complicated geometry, so it is natural to look to the finite element method (FEM) for a solution. Of course, the accuracy of the FEM is determined mainly by the element model. A few authors [26-33] have developed finite element techniques to predict the performance of constrained-layer damped shell structures of general shape. Johnson et al. [27, 28] developed a three-dimensional model using the MSC/NASTRAN computer program. Soni [29] developed a three-layer shell element and compared this with results from both the MSC/NASTRAN program and an analytical method. Other contributions in this area are by Ahmed [30], Sainsbury and Ewins [31], S, and Bisco [32] An earlier review on this subject can be found in various references by Nakra [33].

2.4 Complex behavior of viscoelastic materials and Complex modulus models:

Polymeric materials are widely used for sound and vibration damping. One of the more notable properties of these materials, besides the high damping ability, is the strong frequency dependence of dynamic properties; both the dynamic modulus of elasticity and the damping characterized by the loss factor.

Mycklestad [34] was one of the pioneering scientists into the investigation of complex modulus behavior of viscoelastic materials (Jones, 2001, Sun, 1995). Viscoelastic material properties are generally modeled in the complex domain because of the nature of viscoelasticity. Viscoelastic materials possess both elastic and viscous properties. The typical behavior is that the dynamic modulus increases monotonically with the increase of frequency and the loss factor exhibits a wide peak [3, 35]. It is rare that the loss factor peak, plotted against logarithmic frequency, is symmetrical with respect to the peak maximum, especially if a wide frequency range is considered. The experiments usually reveal that the

peak broadens at high frequencies. In addition to this, the experimental data on some polymeric damping materials at very high frequencies, far from the peak centre, show that the loss factor–frequency curve ‘‘flattens’’ and seems to approach a limit value, while the dynamic modulus exhibits a weak monotonic increase at these frequencies [36-41]. These phenomena can be seen in the experimental data published by Madigosky and Lee [36], Rogers [37] and Capps [38] for polyurethanes, and moreover by Fowler [39], Nashif and Lewis [40], and Jones [41], for other polymeric damping materials.

The computerized methods of acoustical and vibration calculus require the mathematical form of frequency dependences of dynamic properties. A reasonable method of describing the frequency dependences is to find a good material model fitting the experimental data. The introduction of fractional calculus into the model theory of viscoelasticity has resulted in a powerful tool to model the dynamic behavior of polymers and other materials [37, 42-54]. In this way, the quantitative behavior of the conventional viscoelastic models (Kelvin, Maxwell, Zener, etc.) can be improved, and a number of fractional derivative models can be developed. Of these models, the fractional derivative Zener model characterized by four parameters has proved to be especially appropriate to predict the dynamic behavior of polymeric damping materials over a wide frequency range [37, 41, 51]. This model is robust and has solid theoretical basis [41], but is not able to describe the asymmetry of the loss peak and the high-frequency behavior of the dynamic properties outlined above.

Modelling the asymmetrical loss peak is an old problem not only in polymer mechanics, but also in the field of dielectric properties of polymers. For this purpose, empirical models—mathematical formulae—have been developed which can be used in describing either the dielectric or the dynamic mechanical properties of polymers [55]. Among the models, the Havriliak–Negami model is especially useful and has been used intensively for the asymmetrical loss factor peak of polymeric damping materials, mainly polyurethanes [56]. Nevertheless, the Havriliak–Negami model cannot describe the aforementioned high-frequency behavior of the polymeric damping materials, since this model predicts a vanishing loss factor and a finite limit value for the dynamic modulus at high frequencies. The other disadvantage of this empirical model is that it cannot be related to the general

constitutive equation of viscoelastic materials. One of the fractional derivative models, used by Bagley and Torvik [43], is free from these disadvantages and able to predict an asymmetrical loss peak, but this fractional model is not correct theoretically [44]. Later Friedrich and Braun [47], suggested another empirical formula for asymmetrical loss peak.

Chapter 3

Modeling and Applications of Viscoelastic Treatments and Materials

3.1 Typical Applications and Viscoelastic Material Characteristics

Many polymers exhibit viscoelastic behavior. Viscoelasticity is a material behavior characteristic possessing a mixture of perfectly elastic and perfectly viscous behavior. An elastic material is one in which there is perfect energy conversion, that is, all the energy stored in a material during loading is recovered when the load is removed. Thus, elastic materials have an in phase stress-strain relationship. Figure 3.1a illustrates this concept. Contrary to an elastic material, there exists purely viscous behavior, illustrated in Figure 3.1b. A viscous material does not recover any of the energy stored during loading after the load is removed (the phase angle between stress and strain is exactly π/2 radians).

All energy is lost as 'pure damping.' For a viscous material, the stress is related to the strain as well as the strain rate of the material. Viscoelastic materials have behavior which falls between elastic and viscous extremes. The rate at which the material dissipates energy in the form of heat through shear, the primary driving mechanism of damping materials, defines the effectiveness of the viscoelastic material.

Because a viscoelastic material falls between elastic and viscous behavior, some of the energy is recovered upon removal of the load, and some is lost or dissipated in the form of thermal energy. The phase shift between the stress and strain maximums, which does not to exceed 90 degrees, is a measure of the materials damping performance. The larger the phase angle between the stress and strain during the same cycle (see Figure 3.1c), the more effective a material is at damping out unwanted vibration or acoustical waves.

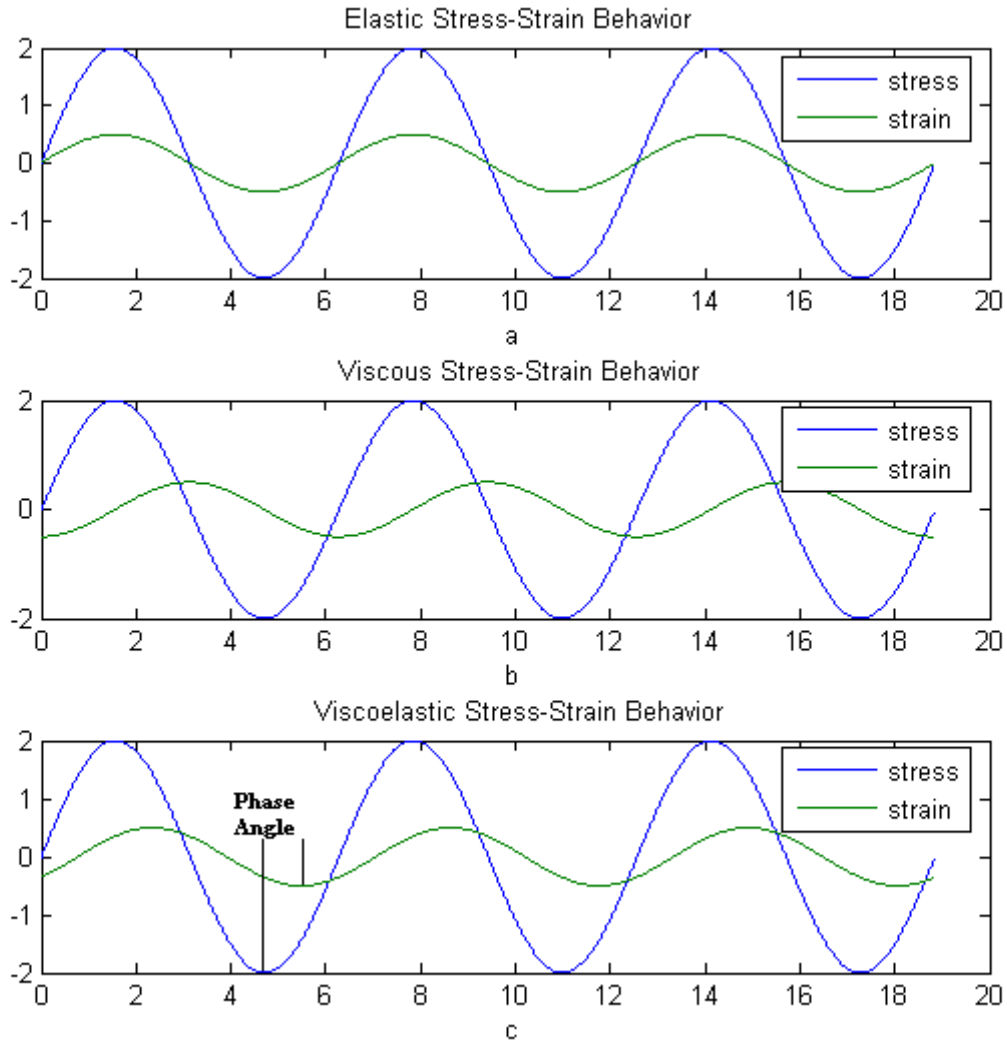

Figure 3.1. a) Elastic stress-strain behavior. **B)** Viscous stress-strain behavior. **c)** Viscoelastic stress-strain behavior

Because viscoelastic materials are generally polymers, there is enormous variability in the composition of viscoelastic materials. This will be discussed in more detail in relation to properties of viscoelastic materials, namely complex moduli, in section 3.1.1, but some typical materials which are used for damping are presented in Table 3.1

Table 3.1 List of common viscoelastic polymeric materials
(Jones, "Handbook of Viscoelastic Damping," 2001)

1. Acrylic Rubber
2. Butadiene Rubber
3. Butyl Rubber
4. Chloroprene
5. Chlorinated Polyethylene
6. Ethylene-Propylene-Diene
7. Fluorosilicone Rubber
8. Fluorocarbon Rubber
9. Nitrile Rubber
10. Natural Rubber
11. Polyethylene
12. Polystyrene
13. Polyvinyl chloride (PVC)
14. Polymethyl Methacrylate (PMMA)
15. Polybutadiene
16. Polypropylene
17. Polyisobutylene
18. Polyurethane
19. Polyvinyl acetate
20. Polyisoprene
21. Styrene-butadiene (SBR)
22. Silicon Rubber
23. Urethane Rubber

Viscoelastic polymers are generally used for low amplitude vibration damping such as damping of sound transmission and acoustical waves through elastic media. Some typical applications of the polymers presented in Table 3.1 are shown in Table 3.2.

Table 3.2. Some common applications for viscoelastic materials

Common Viscoelastic Materials Application
Grommets or Bushings
Component Vibration Isolation
Aircraft fuselage Panels
Submarine Hull Separators
Mass Storage Disk Drive Component
Automobile Tires
Stereo Speakers
Bridge Supports
Caulks and Sealants
Lubricants
Fiber Optics Compounds
Electrical and Pumping

3.2 Modeling of Viscoelastic Materials

Unlike structural components which exhibit fairly straight-forward dynamic response, viscoelastic materials are somewhat more difficult to model mathematically. Because most high load bearing structures tend to implement high strength metal alloys, which usually

have fairly straight-forward stress-strain and strain-displacement relationships, the dynamics of such structures are simple to formulate and visualize.

An engineer or analyst need only take into account the varying geometries of these structures and the loads which are applied to them to accurately model the dynamics because the material properties of the structure and its components are generally well known. However, difficulty arises when viscoelastic materials are applied to such structures. This difficulty is mainly due to the strain rate (frequency), temperature, cyclic strain amplitude, and environmental dependencies between the viscoelastic material properties and their associated effect on a structure's dynamics (Jones, 2001, Sun, 1995). Additionally, many viscoelastic materials and the systems to which they are applied exhibit nonlinear dynamics over some ranges of the aforementioned dependencies, further complicating the modeling process (Jones, 2001).

3.2.1 Properties of Viscoelastic Materials

Mycklestad [34] was one of the pioneering scientists into the investigation of complex modulus behavior of viscoelastic materials (Jones, 2001) [2]. Viscoelastic material properties are generally modeled in the complex domain because of the nature of viscoelasticity. As previously discussed, viscoelastic materials possess both elastic and viscous properties. The moduli of a typical viscoelastic material are given in equation set

$$E^* = E' + iE'' = E'(1 + i\eta)$$
$$G^* = G' + G'' = G'(1 + i\eta) \quad \text{---------- (3.1)}$$

Where the '*' denotes a complex quantity. In equation set (3.1), as in the rest of this report, E and G are equivalent to the elastic modulus and shear modulus, respectively. Thus, the moduli of a viscoelastic material have an imaginary part, called the loss modulus, associated with the material's viscous behavior, and a real part, called the storage modulus, associated with the elastic behavior of the material. This imaginary part of the modulus is also

sometimes called the loss factor of the material, and is equal to the ratio of the loss modulus to the storage modulus. The real part of the modulus also helps define the stiffness of the material. Furthermore, both the real and imaginary parts of the modulus are temperature, frequency (strain rate), cyclic strain amplitude, and environmentally dependent.

3.2.1.1 Temperature Effects on the Complex Modulus

The properties of polymeric materials which are used as damping treatments are generally much more sensitive to temperature than metals or composites. Thus, their properties, namely the complex moduli represented by E, G, and the loss factor h , can change fairly significantly over a relatively small temperature range. There are three main temperature regions in which a viscoelastic material can effectively operate, namely the glassy region, transition region, and rubbery region (Jones, 2001, Sun, 1995)[2]. Figure 3.2 shows how the loss factor can vary with temperature.

The glassy region is representative of low temperatures where the storage moduli are generally much higher than for the transition or rubbery regions. This region is typical for polymers operating below their brittle transition temperature. However, the range of temperatures which define the glassy region of a polymeric material is highly dependent on the composition and type of viscoelastic material. Thus, different materials can have much different temperature values defining their glassy region. Because the values of the storage moduli are high, this inherently correlates to very low loss factors. The low loss factors in this region are mainly due to the viscoelastic material being unable to deform (having high stiffness) to the same magnitude per load as if it were operating in the transition or rubbery regions where the material would be softer. On the other material temperature extreme, the rubbery region is representative of high material temperatures and lower storage moduli. However, though typical values of storage moduli are smaller, like the glassy region the material loss factors are also typically very small. This is due to the increasing breakdown of material structure as the temperature is increased. In this region, the viscoelastic material is easily deformable, but has lower interaction between the polymer chains in the structure of the material.

Cross-linking between polymer chains also becomes a less significant property as temperature is increased. A lower interaction between the chains results in the material taking longer to reach equilibrium after a load is removed. Eventually, as the temperature hits an upper bound critical value (also known as the flow region temperature), the material will begin to disintegrate and have zero effective loss factor and zero storage modulus.

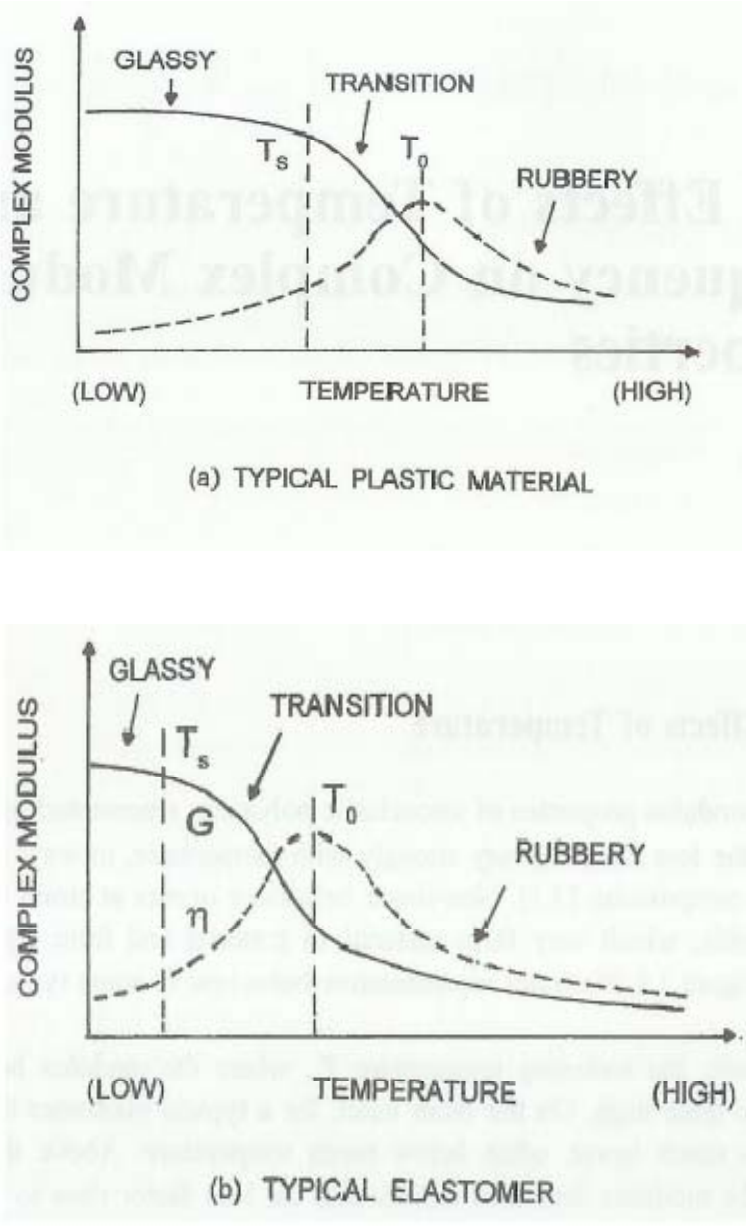

Figure 3.2. Temperature effects on complex modulus and loss factor material properties (Jones, "Handbook of Viscoelastic Damping," 2001).

The region falling between the glassy and rubbery regions is known as the transition region. Materials which are used for practical damping purposes generally should be used within this region because loss factors rise to a maximum. In more detail, if a material is within the glassy region and the temperature of the material is increased, the loss factor will rise to a maximum and the storage modulus will fall to an intermediate value within the transition region. As the material temperature is further increased into the rubbery region, the loss factor will begin to fall with the storage modulus. This behavior is illustrated in Figure 3.2. Therefore, it is extremely important to know the operating temperature range during the design phase of a host structure to which a viscoelastic damping treatment will be applied so that the viscoelastic treatment will be maximally effective.

3.2.1.2 Frequency Effects on the Complex Modulus

Like temperature, frequency also has a profound effect on the complex modulus properties of a viscoelastic polymer, though to a much higher degree with an inverse relationship. The three regions of temperature dependence (glassy, transition, rubbery) can sometimes be a few hundred degrees, more than covering a typical operational temperature range of an engineered structure. But the range of frequency within a structure can often be several orders of magnitude. The frequency dependence on complex moduli can be significant from as low as 8 10−Hz to 8 10 Hz, a range much too wide to be measured by any single method (Jones, 2001) [2]. Furthermore, relaxation times after deformation of a viscoelastic material can be anywhere from nanoseconds to years and will greatly effect one's measurement methods, especially at low temperatures.

Frequency has an inverse relationship to complex moduli with respect to temperature. At low frequency, the storage moduli are low and the loss factors are low. This region is synonymous with the rubbery region (high temperatures). This is due to the low cyclic strain rates within the viscoelastic layer. As the frequency is increased, the material hits the transition region where the loss factor hits a maximum value. As the frequency is increased further, the storage moduli increase as the loss factor decreases. Thus, the transition region is

again the range of frequency for which a material should be chosen to correspond to a host structure's typical operating range. Figure 4.3 illustrates this behavior.

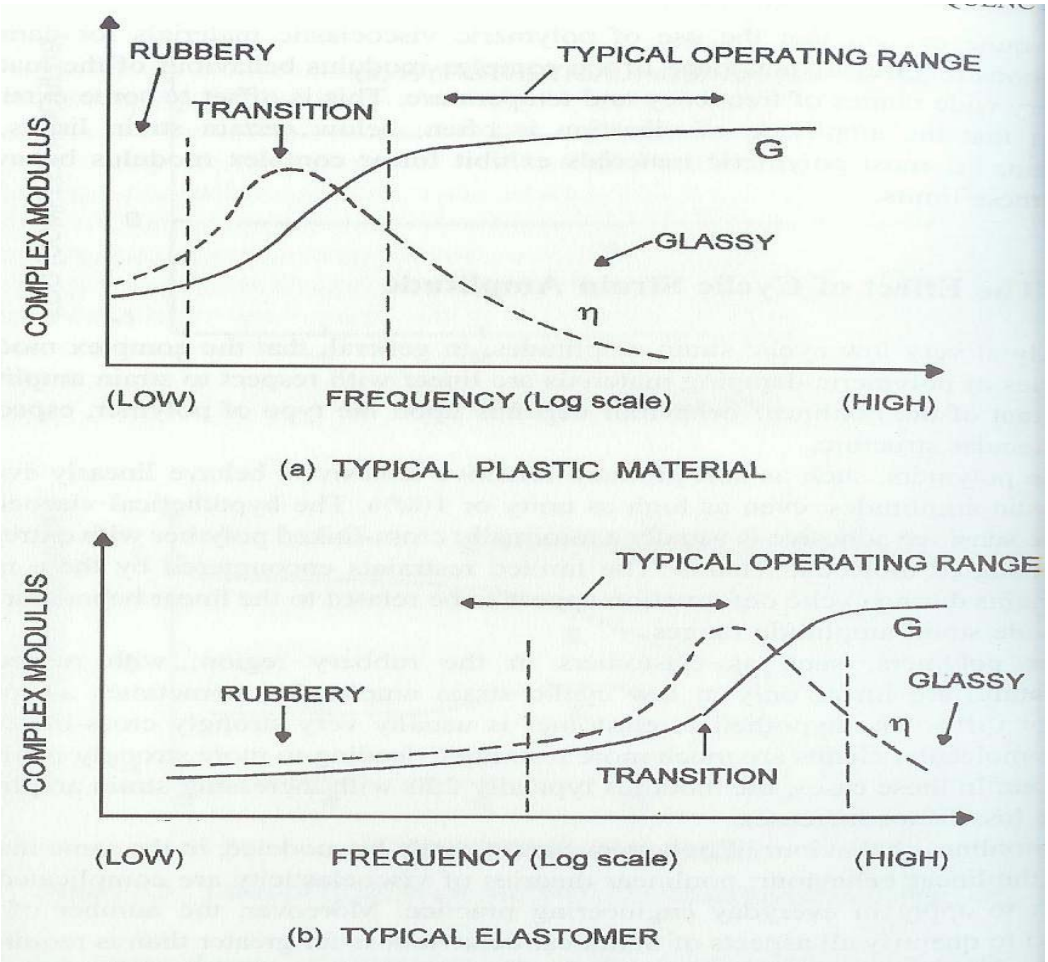

Figure 3.3. Frequency effects on complex modulus and loss factor material properties (Jones, "Handbook of Viscoelastic Damping," 2001).

3.2.1.3 Cyclic Strain Amplitude Effects on Complex Modulus

The effect of cyclic strain amplitude on polymeric complex moduli is highly dependent on the composition and type of the polymer, particularly the molecular structure (Jones, 2001, Sun, 1995). Experiments have shown that the complex moduli of polymers generally behave linearly only at low cyclic strain amplitudes (Jones, 2001). There are, however, polymers such as pressure sensitive adhesives, which exhibit linearity even at high cyclic strain

amplitudes. These polymers usually have very few cross links between long, entangled polymer chains. Therefore, the low interaction between these chains seems to have an effect on the linear behavior over wide strain amplitude ranges (Jones, 2001). However, most viscoelastic polymers used in typical damping applications behave nonlinearly at high strain amplitudes. This nonlinearity is very difficult to model accurately and involves very complicated theories and a significant number of tests, many more than for linear complex modulus behavior, to gather data sufficient to establish trends for a specific material (Jones, 2001, Sun, 1995).

3.2.1.4 Environmental Effects on Complex Modulus

The environment plays a significant role in all outdoor engineering applications. Temperature ranges, climate, amount of rainfall or direct exposure to sunlight, as well as foreign substance exposure (such as petroleum products, alkalis, harmful chemicals, etc.) are necessary design factors to take into consideration for any outdoor engineering project. The same holds true when considering applying a viscoelastic treatment to an engineered structure. Temperature dependence on the behavior of viscoelastic complex moduli has already been discussed. But depending on the application, polymer type, and composition of the material, exposure to foreign substances must also be addressed.

Oils and other patrols can penetrate into some materials and alter the behavior as well as jeopardize the bond between a material and the host structure, something which will be shown to be very important. Therefore, it is important to study the effects of these foreign elements on the behavior of the material which will be used in a particular application. Some elements may be more important than others depending on the operating environment, so these elements should hold the highest interest of the designer.

Chapter 4

Analytical Mathematical Models and Viscoelastic Theory

4.1 Classic viscoelastic models:

In the past, many simple models of viscoelastic behavior have been based on combinations of elastic and viscous elements, ranging from basic discrete systems such as the Maxwell and Voigt models [2] to distribution of infinite numbers of such elements. The complex stiffness of the Maxwell model is calculated by adding two effective stiffnesses in the series to give:

$$k^* = k(1+i\eta) = \frac{i\omega k_1 c_1}{k_1 + i\omega c_1} \qquad \text{---------- (4.1)}$$

Where c_1 is the dashpot coefficient and k_1 is the stiffness of the element .On the other hand, the stiffness of the Voigt model is equal to the sum of two effective stiffnesses (k_2 and ωc_2) in parallel:

$$k^* = k(1+i\eta) = k_2 + i\omega c_2 \qquad \text{---------- (4.2)}$$

And the complex stiffness of the standard model, being the sum of a Voigt and a Maxwell element in parallel, is:

$$k^* = k(1+i\eta) = \frac{i\omega k_1 c_1}{k_1 + i\omega c_1} + k_2 + i\omega c_2 \qquad \text{---------- (4.3)}$$

4.2 The fractional derivative model

4.2.1 The time-domain equations

A great simplification in modeling viscoelastic material behavior has been recognized in recent years, particularly with respect to the frequency domain, by using fractional derivative models instead of the classical approach. The fractional derivative model appears to be more complicated at first sight but, but provides much less rapid variation of the complex modulus properties with frequency.

The viscoelastic behavior of polymers in the time domain is far more complicated than for the frequency domain. One approach to time domain analysis is to use the Fourier Transform to return from the frequency domain in to the time domain, usually by means of numerical integration. In the fractional derivative model, the relationship between extensional stress and extensional strain is described, for the first order case by the relationships:

$$\tau(t) + c_1 D^{\beta}\tau(t) = a_1\phi(t) + b_1 D^{\beta}\phi(t)$$
$$\sigma(t) + c_1 D^{\beta}\sigma(t) = a_1\varepsilon(t) + b_1 D^{\beta}\varepsilon(t) \quad \text{---------- (4.4)}$$

Where, for example, $D^{\beta}\sigma(t)$ is the βth order fractional derivative of the stress σ(t),
Defined by:

$$D^{\beta}\sigma(t) = \frac{1}{\Gamma(1-\beta)}\frac{d}{dt}\int_0^t \frac{\sigma(\tau)}{(t-\tau)^{\beta}}dt \quad \text{---------- (4.5)}$$

Where $\Gamma(x)$ is the Gamma function of argument x.

4.2.2 Application to the frequency domain

The frequency domain model is even more useful in the frequency domain and much easier to apply. If, for example, the strain is defined as $\varepsilon(t) = \varepsilon_0 \exp(i\omega t)$ and the stress as $\sigma(t) = \sigma_0 \exp(i\omega t)$, in the case of extensional deformation, then the equation (4.4) and (4.5) reduce to the much simpler form :

$$\sigma = \frac{[a_1 + b_1(i\omega^{\beta})]}{[1 + c_1(i\omega^{\beta})} \varepsilon \quad \text{---------- (4.6)}$$

So that the complex modulus E* is simply:

$$E^* = E(1 + i\eta) = \frac{[a_1 + b_1(i\omega^{\beta})]}{[1 + c_1(i\omega^{\beta})} \quad \text{---------- (4.7)}$$

Further more in accordance with the frequency-temperature equivalence principle, ω can be replaced by the reduced frequency $2\pi f\ \alpha(T)$, where f in the frequency in Hz and α(T) depends upon the temperature, provided that appropriate values of the parameter are selected , so that in the most general case:

$$E^* = \frac{a_1 + b_1(2\pi f\ \alpha(T)^{\beta}}{1 + c_1(2\pi f\ \alpha(T)^{\beta})} \quad \text{---------- (4.8)}$$

In this equation E* is the complex number and a_1 and b_1 may or may not be complex.

There have been several analytical methods developed since the late 1950's to predict response of damped systems. Some of the more popular methods include those developed by Ross, Kerwin, and Ungar (Ross, 1959) [5], Mead and Markus (Mead, 1969) [8], DiTaranto (DiTaranto, 1965) [7], Yan and Dowell (Yan, 1972),[11] and Rao and Nakra (Rao, 1974) [15]. However, the development of finite element software has increased the accuracy and precision of estimations of the dynamic responses of damped structures. For fairly simple

structures, analytical methods can be used as a substitution for finite element predictions. Furthermore, finite element packages are often computationally expensive, something that might not be needed for damping predictions of simpler systems. In this case, a simple code or program can be written implementing an analytical method to derive a simple, sufficiently accurate damping model. As the complexity of the system increases, however, finite element formulations should be strongly considered as the boundary conditions and system parameters may prove too difficult to define using a simple analytical based formulation.

4.3 Ross, Kerwin, and Ungar Damping Model

Ross, Kerwin, and Ungar [5], developed one of the earliest damping models for three layered sandwich beams based on damping of flexural waves by a constrained viscoelastic layer. They employed several major assumptions, including (Sun, 1995):

- For the entire composite structure cross section, there is a neutral axis whose location varies with frequency.
- There is no slipping between the elastic and viscoelastic layers at their Interfaces.
- The major part of the damping is due to the shearing of the viscoelastic material, whose shear modulus is represented by complex quantities in terms of real shear moduli and loss factors.
- The elastic layers displaced laterally the same amount.
- The beam is simply supported and vibrating at a natural frequency or the beam is infinitely long so that the end effects may be neglected.

These assumptions apply to any constrained layer damping treatment applied to a rectangular beam. Figure 4.1 shows an example system which the Ross, Kerwin, and Ungar (RKU) equations could be applied to. This laminate beam system is also the layup for the cantilever beam used for materials testing later in this report.

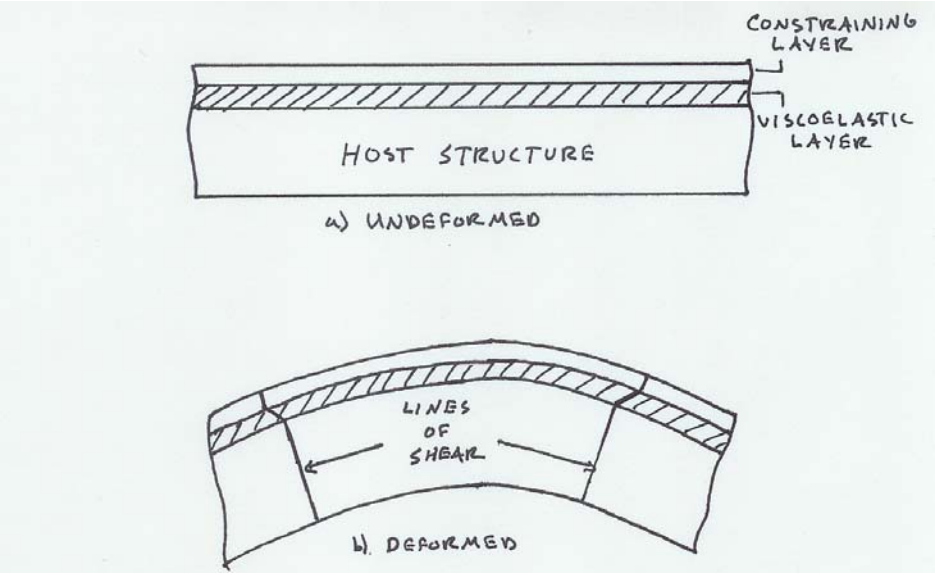

Figure 4.1. Three layer cantilever beam with host beam, viscoelastic layer, and constraining layer clearly defined.

Comparison between experimental data and this theory have shown that results from theory correlate well to experiment (Ross, 1959). The model is represented by a complex flexural rigidity, (EI)*, where the '*' denotes a complex quantity, given by:

$$(EI)^* = \frac{E_s h_s^3}{12} + \frac{E_v^* h_v^3}{12} + \frac{E_c h_c^k}{12} - \frac{\frac{E_v h_c^2}{12}(d-D)}{(1+g_v^*)} + E_s h_s D^2 + E_v^* h_v (h_{vs} - D)^2 + E_c h_c (d-D)^2 - \left[\frac{E_v^* h_v (h_v^s - D)}{2} + E_c h_c (d-D)\right]\left[\frac{(d-D)}{(1+g_v^*)}\right] \quad \text{---------- (4.6)}$$

where D is the distance from the neutral axis of the three layer system to the neutral axis of the host beam,

$$D = \frac{E_v^* h_v (h_{vs} - \frac{d}{2}) + g_v^* (E_v^* h_v h_{vs} + E_c h_c d)}{E_s h_s + \frac{E_v^* h_v}{2} + g_v^* (E_s h_s + E_v^* h_s + E_c h_c)}$$

$$h_{vs} = \frac{h_s + h_v}{2}$$

$$g_v^* = \frac{G_v^*}{E_c h_c h_v p_1^2}$$

$$d = h_v + \frac{h_s + h_c}{2}$$

---------- (4.7)

In these equations E_s, E^*_v, E_c and h_s, h_v, h_c are the elastic moduli and thicknesses of the host structure, viscoelastic layer, and constraining layer, respectively. The term g^*_v is known as the 'shear parameter' which varies from very low when G^*_v is small to a large number when G^*_v is large. The term 'p' within the shear parameter is the wave number, namely the n^{th}, eigen value divided by the beam length. The shear parameter can also be expressed in terms of modal frequencies by:

$$g_v^* = \frac{G_v^* L^2}{E_c h_v h_c \xi_n^2 \sqrt{c_n}}$$

$$\xi_n^4 = \frac{\rho_s b h_s \omega_n^2 L^4}{E_s I_s}$$

---------- (4.8)

Where ω_n is the n^{th} modal frequency and C_n are correction factors determined by Rao(Rao, 1974) and are given in Table 4.1.

Table 4.1. Rao correction factors for shear parameter in RKU equations (Jones, "Handbook of Viscoelastic Damping," 2001).

Boundary conditions	Correction factors	
	Mode 1	Mode2
Pined-pined	1	1
Clamped-clamped	1.4	1
Clamped-pined	1	1
Clamped-free	0.9	1
Free-free	1	1

Chapter 5

Formulation Using Finite Element Method

5.1 The displacement description

The finite element model of the damped three-layer beam is shown in Fig. 5.1. It is assumed that every layer has the same transverse displacement, as has been proved by both numerical and experimental analysis [26, 27, 31], and that the deformation of the face sheets obeys thin plate theory.

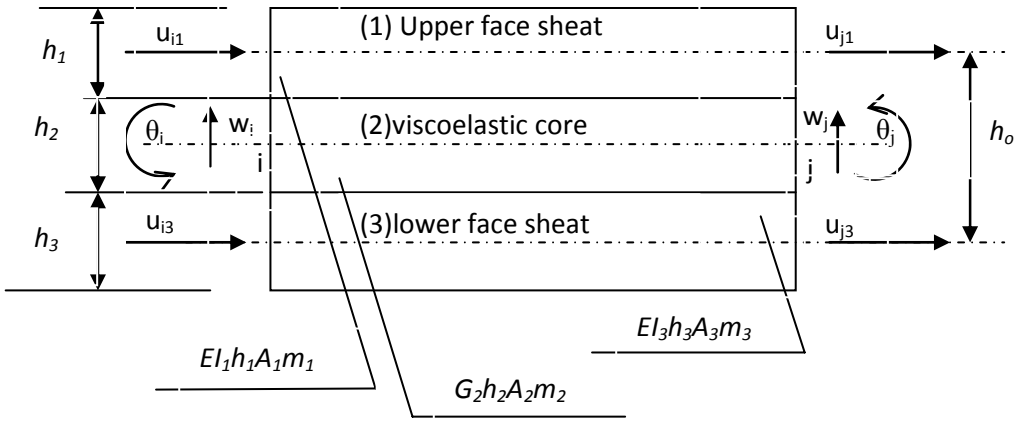

Fig 5.1 Finite element model for the damped sandwich beam (where A_i and m_i are the cross sectional area and mass per unit length of the i^{th} layer of the beam element).

At each node n, four displacements $\{\mathbf{q}_n\}$ are introduced, these being the transverse displacement ω_n, the rotation θ_n of the elastic layers (or face sheets), and the axial displacements u_{n1},u_{n3} of the middle planes of these face sheets. The total set of nodal displacements for the element is:

$$\{q^e\} = \begin{Bmatrix} q_i \\ q_j \end{Bmatrix} = [w_i \quad \theta_i \quad u_{1i} \quad u_{1j} \quad w_j \quad \theta_j \quad u_{3i} \quad u_{3j}] \text{ ---------- (5.1)}$$

With the traditional polynomial shape functions, the displacement field vector {δ} may be written as

$$\begin{Bmatrix} w \\ \theta \\ u_1 \\ u_3 \end{Bmatrix} = \begin{bmatrix} N_f \\ N'_f \\ N_1 \\ N_3 \end{bmatrix} = \{q^e\} \qquad \text{---------- (5.2)}$$

Where

[N1] = { 0 0 1-ζ 0 0 0 ζ 0 }

[N3] = { 0 0 0 1-ζ 0 0 0 ζ }

[Nf] = { 1-3ζ2+2ζ (ζ- 2ζ2+ζ3)L 0 0 3ζ2-2ζ3n (-ζ2+ ζ2)L 0 0 }

$$[N'_f] = \left[\frac{\partial Nf}{\partial x}\right] = \left[\frac{1}{L}\frac{\partial Nf}{\partial x}\right] \qquad \text{---------- (5.3)}$$

ζ = x/L, L = element length

5.2 Stiffness matrix for the face sheets

The stiffness matrix for the elastic face sheets may be obtained from the bending and extensional strain energies as follows:

$$U_{be} = \frac{1}{2}\int_V (\varepsilon_1\sigma_1 + \varepsilon_3\sigma_3)dV$$

$$= \frac{1}{2}\int_0^L \left(E_1A_1\left(\frac{\partial u_1}{\partial x}\right)^2 + E_3A_3\left(\frac{\partial u_3}{\partial x}\right)^2 + (E_1I_1 + E_3I_3)\left(\frac{\partial^2 w}{\partial x^2}\right)^2 \right) dx$$

$$= \frac{1}{2}\{q^e\}^T \int_0^1 \left(\frac{E_1 L_1}{L}[N_1']^{T_t}[N_1'] + \frac{E_3 L_3}{L}[N_3']^T[N_3'] + \frac{EI}{L^3}[N_f'']^T[N_f''] \right) d\xi \{q^e\}$$

$$= \frac{1}{2}\{q^e\}^T [K_{qq}]_{be}^e \{q^e\} \qquad \text{---------- (5.4)}$$

$$[K_{qq}]_{be}^e = \begin{bmatrix} \frac{12EI}{L^3} & & & & & & & \\ \frac{6EI}{L^2} & \frac{4EI}{L} & & & & & & \\ 0 & 0 & \frac{E_1 A_1}{L} & & & & & \\ 0 & 0 & 0 & \frac{E_3 L_3}{L} & & & & \\ -\frac{12EI}{L^3} & -\frac{6EI}{L^2} & 0 & 0 & \frac{12EI}{L^3} & & & \\ \frac{6EI}{L^3} & \frac{2EI}{L} & 0 & 0 & -\frac{6EI}{L^2} & \frac{4EI}{L} & & \\ 0 & 0 & -\frac{E_1 A_1}{L} & 0 & 0 & 0 & \frac{E_1 A_1}{L} & \\ 0 & 0 & 0 & -\frac{E_3 A_3}{L} & 0 & 0 & 0 & \frac{E_3 A_3}{L} \end{bmatrix}$$

---------- (5.5)

Where $EI = E_1 L_1 + E_3 L_3$

5.3 Stiffness matrix for the core layer

The stiffness matrix of the constrained damping layer can be obtained from its shear strain energy. Here the bending and extensional strain energies are ignored due to their second-order smallness compared with the shear strain energy. It can be seen from Fig.5.2 that the shear strain is given by

$$-\gamma_2 = \frac{u_1 - u_3}{h_2} + \frac{h_0}{h_2}\theta = \frac{u_1 - u_3}{h_2} + \frac{h_0}{h_2}\frac{dw}{dx} \qquad \text{---------- (5.6)}$$

$$\gamma_2 = -\left[\frac{N_1 - N_3}{h_2} + \frac{h_0}{h_2}\frac{dN_f}{dx}\right]\{q^e\} \qquad \text{---------- (5.7)}$$

$$U_{shear} = \frac{1}{2}\int_V G_2\gamma_2^2 dV$$

$$= \frac{1}{2}\frac{G_2 A_2 L}{h_2^2}\{q^e\}^T \int_0^1 \left[N_1 - N_3 + \frac{h_0}{L}N_f'\right]^T \left[N_1 - N_3 + \frac{h_0}{L}N_f'\right] d\xi \{q^e\}$$

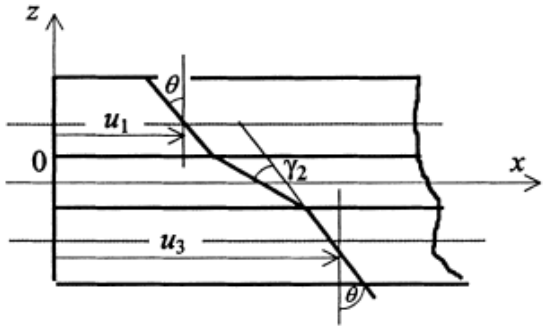

Fig. 5.2. The shear strain of the damping layer.

$$U_{shear} = \frac{1}{2}\{q^e\}^T [K_{qq}]^e_{shear}\{q^e\} \qquad \text{---------- (5.8)}$$

$$[K_{qq}]^e_{shear} = \frac{G_2 A_2 L}{h_2^2} \times \begin{bmatrix} \frac{6h_0^2}{5L^2} & & & & & & & \\ \frac{h_0^2}{10L} & \frac{2h_0^2}{15} & & & & & & \\ \frac{-h_0}{2L} & \frac{h_0}{12} & \frac{1}{3} & & & & & \\ \frac{h_0}{2L} & \frac{-h_0}{12} & \frac{-1}{3} & \frac{1}{3} & & & & \\ \frac{6h_0^2}{5L^2} & \frac{-h_0^2}{10L} & \frac{h_0}{2L} & \frac{-h_0}{2L} & \frac{6h_o^2}{5L^2} & & & \\ \frac{h_0^2}{10L} & \frac{-h_0^2}{30} & \frac{-h_0}{12} & \frac{h_0}{12} & \frac{-h_0^2}{10L} & \frac{2h_0^2}{15} & & \\ \frac{-h_0}{2L} & \frac{-h_0}{12} & \frac{1}{6} & \frac{-1}{6} & \frac{-h}{2L} & \frac{h_0}{12} & \frac{1}{3} & \\ \frac{h_0}{2L} & \frac{h_0}{12} & \frac{-1}{6} & \frac{1}{6} & \frac{-h_0}{2L} & \frac{-h_0}{12} & \frac{-1}{3} & \frac{1}{3} \end{bmatrix}$$

---------- (5.9)

5.4 The element stiffness matrix

The complete stiffness matrix for the element is obtained from Eqs. (5) and (9) as

$$[K_{qq}]^e = [K_{qq}]^e_{be} + [K_{qq}]^e_{shear}$$ ---------- (5.10)

5.5 The element mass matrix

Following a similar procedure, the mass matrix for the sandwich beam element is obtained from the kinetic energy as follows:

$$T = \frac{1}{2}\int_0^L \left(m_0 \dot{w}^2 + m_1 \dot{u}_1^2 + m_3 \dot{u}_3^2\right) dx$$

$$= \frac{L}{2}\{\dot{q}^e\}^T \int_0^1 \left(m_0 [N_f]^T [N_f] + m_1 [N_1]^T [N_1] + m_3 [N_3]^T [N_3] \right) d\xi \{\dot{q}^e\}$$

$$= \frac{1}{2}\{\dot{q}^e\}^T [M_{qq}]^e \{\dot{q}^e\}$$ ---------- (5.11)

Then we have

$$[M_{qq}]^e = \int_0^1 \left(m_0 [N_f]^T [N_f] + m_1 [N_1]^T [N_1] + m_3 [N_3]^T [N_3] \right) d\xi$$

$$= \begin{bmatrix}
\frac{13m_0L}{35} & & & & & & & \\
\frac{11m_0L^2}{210} & \frac{m_0L^3}{105} & & & & & & \\
0 & 0 & \frac{m_1L}{3} & & & & & \\
0 & 0 & 0 & \frac{m_3L}{3} & & & & \\
\frac{9m_0L}{70} & \frac{13m_0L^2}{140} & 0 & 0 & \frac{13m_0L}{35} & & & \\
-\frac{13m_0L^2}{420} & -\frac{m_0L^3}{140} & 0 & 0 & -\frac{11m_0L^2}{210} & \frac{m_0L}{105} & & \\
0 & 0 & \frac{m_1L}{6} & 0 & 0 & 0 & \frac{m_1L}{3} & \\
0 & 0 & 0 & -\frac{m_3L}{6} & 0 & 0 & 0 & \frac{m_3L}{3}
\end{bmatrix}$$

---------- (5.12)

Where $m_0 = m_1 + m_2 + m_3$, m_1 is the mass per unit length of the *i*th layer of the beam element.

Chapter 6

Experimental Determination of Viscoelastic Material Properties

The stress-strain relationship for a viscoelastic material under cyclic loading takes on the form of an ellipse shown in Figure 6.1.

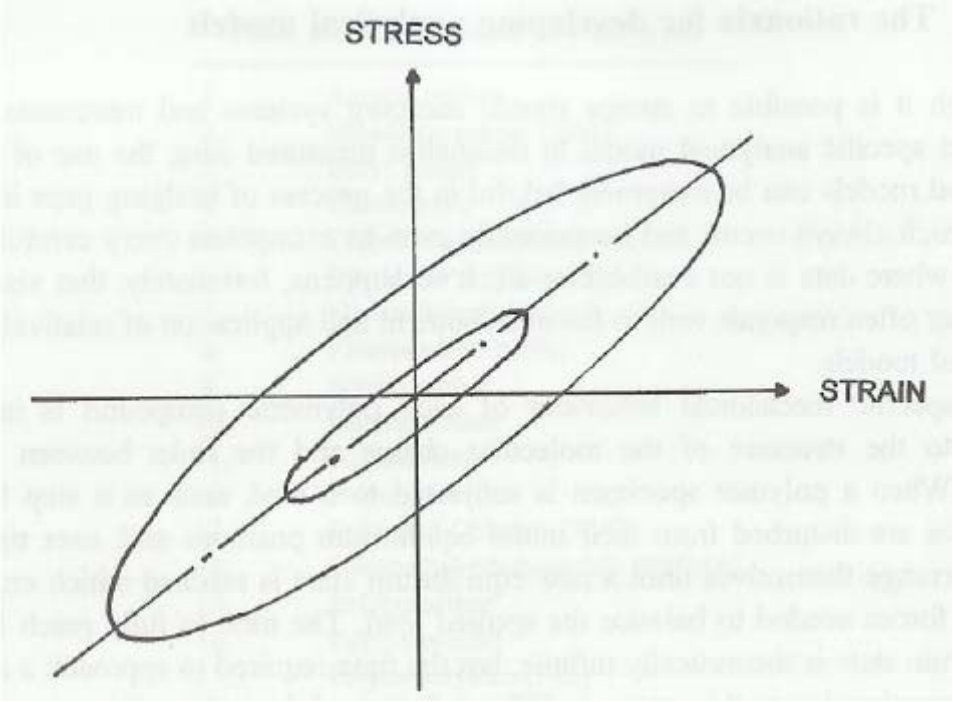

Fig 6.1 Stress-Strain hysteresis loop for linear viscoelastic material

(Jones, "Handbook of Viscoelastic Damping," 2001).

The stress-strain relationship for a linear viscoelastic material is given by

$$\sigma = (E' + E'')\varepsilon = E'\varepsilon + \frac{E''}{|\omega|}\frac{d\varepsilon}{dt} \quad \text{---------- (6.1)}$$

since $i|\omega|\varepsilon = \frac{d\varepsilon}{dt}$ for harmonic motion (Sun, 1995). Again, note the strain rate, or frequency, dependence on the stress within the viscoelastic material not found in stress strain relationships for metals in the elastic region. As mentioned, above the loss factor is the ratio of loss modulus (imaginary part of the complex modulus) to the storage modulus (real part of complex modulus). In the above equation, E' represents storage modulus, synonymous with the elastic modulus for metals. Sun and Lu explain that the area enclosed by the ellipse in Figure 6.1 is equal to the energy dissipated by the viscoelastic material per loading cycle. Additionally, the slope of the major axis of the ellipse in Figure 6.1 is representative of the storage modulus of the viscoelastic material. Thus, E' is easily found from the hysteresis plot of stress and strain.

From Figure 6.1, it should be noted that the general shape of the ellipse does not change for small variations of the maximum strain amplitude, ε^0. However, the shape does change as the loss factor changes (i.e. the inner ellipse and outer ellipse in Figure are tests at the same frequency but different strain amplitudes). Thus, the ratio of the minor axis to major axis of the ellipse can be used as a measure of damping (Jones, 2001). However, this ratio is not the loss factor of the material. To find the loss factor of the material, the data generated using the cyclic loading machine can be used to find the energy dissipated per cycle of loading for each viscoelastic material. The energy dissipated is given by the path integral

$$W_d = \oint \sigma d\varepsilon = \int_0^{2\pi/\omega} \sigma \frac{d\varepsilon}{dt} dt = \pi E'' \varepsilon_0^{\,2} \qquad \text{---------- (6.2)}$$

It is also important to find the peak potential energy within the material during a loading cycle. Peak potential energy is given by

$$U = \frac{1}{2} E' \varepsilon_0^2 \qquad \text{---------- (6.3)}$$

From the energy dissipated per cycle and the peak potential energy the loss factor can be found to be

$$\eta = \frac{W_d}{2\pi U} = \frac{E''}{E'} \text{ ---------- (6.4)}$$

Another method of measuring the properties of viscoelastic materials was formulated by Lemerle (Lemerle, 2002), but the analysis used by Sun and Lu is accurate and relatively simple by comparison.

6.1 Modal Analysis of Undamped Cantilever Beam

Prior to each material being tested, the modal frequencies of the undamped cantilever beam must be determined so that a modal analysis prediction of damping can be executed. The following modal analysis was conducted for a beam having a $2x10^{-4}$ m square cross section composed of mild steel ρ = (7860 $\frac{kg}{m^3}$) . The beam was .58 m in length and had a mass per unit length 1.572 $\frac{kg}{m}$.

In this order, once the modal frequencies are known, the materials can be tested at these frequencies, their properties (Moduli and loss factors) determined, and thicknesses of damping layers found using a MATLAB program to predict effective damping at each mode. Lastly, actual tests can be carried out using the thicknesses predicted from MATLAB to find a correlation between theoretical and experimental results.

To find the modal frequencies of an undamped cantilever beam with a tip mass, simple modal analysis can be used. By using a cantilever beam mode shape (Meirovitch) [58].

$$Y_{r(x)} = A_r \sin \beta_r x + B_r \cos \beta_r x + C_r \sinh \beta_r x + D_r \cos \beta_r x \text{ ---------- (6.5)}$$

Where A, B, C, and D are modal constants of each mode shape Y(x), approximated modal frequencies can be found. The parameter β is related to the modal frequency by

$$\beta_r^4 = \frac{\omega_r^2 m}{EI} \qquad \text{---------- (6.6)}$$

By using the boundary conditions of a cantilever beam with a tip mass, namely

Y(0)) = 0

Y'(0)) = 0

Y''(L) =0

$$Y'''(L) = \frac{M}{-mL}\beta^4 Y(L) \qquad \text{---------- (6.7)}$$

with each of these boundary conditions synonymous to the displacement, rotation, moment, and shear within the beam, respectively, a set of four equations can be formulated to solve for the constants A, B, C, and D for each mode. Additionally, these boundary conditions assume that the tip mass has very small rotary inertia compared to the beam. This set of equations is found by differentiating equation (6.5) three times and applying the appropriate boundary condition. The resulting set of equations is

$$\begin{bmatrix} 0 & 1 & 0 & 1 \\ 1 & 0 & 1 & 0 \\ -\sin\beta L & -\cos\beta L & \sinh\beta L & \cos\beta L \\ -\cos\beta L + \bar{M}\beta L\sin\beta L & \sin\beta L + \bar{M}\beta L\cos\beta L & \cosh\beta L + \bar{M}\beta L\sinh\beta L & \sinh\beta L + \bar{M}\beta L\cosh\beta L \end{bmatrix} \begin{Bmatrix} A \\ B \\ C \\ D \end{Bmatrix} = 0$$

---------- (6.8)

In this set of equations $\bar{M} = \frac{M}{mL}$ where M is the mass of the tip mass, m is the mass per unit length of the cantilever beam, and L is the length of the beam. By taking the determinant of the leading matrix in the above equation set and setting that determinant equal to zero, the roots of the resulting sinusoidal equation will yield the b*L* values for which the equation set is satisfied. These roots are the non-trivial solutions which can be used to find the modal frequencies of the cantilever beam If *M* =1, that is the mass at the tip is equal

to the mass of the beam; the resulting modal frequencies are presented in Table 6.1 for the first five modes.

Table 6.1 modal analysis results of undamped cantilever beam

Mode	Beta_L	Modal frequency (rad/s)	Modal frequency (Hz)
1	3.008	116.377	18.522
2	6.894	1045.75	166.437
3	9.657	2051.86	326.565
4	13.526	4025.58	640.691
5	17.40	6663.066	1060.46

6.3 Tested data for some typical damping materials

The tested data [57] for some typical viscoelastic material has been shown as follows:

6.1 Butyl 60A Rubber Testing

Butyl rubber is a synthetic rubber produced by polymerization of about 98% isobutylene with about 2% of isoprene. Butyl rubber is also known as polyisobutylene or PIB. It has excellent impermeability and its long polymer chains give it excellent flex properties. Butyl is often used in making adhesives, agricultural chemicals, fiber optic compounds, caulks and sealants clingfilms, electrical fluids, lubricants such as 2 cycle engine oil, as a gasoline/diesel fuel additive, and even chewing gum. The first major application of butyl was tire inner tubes because of its excellent impermeability to air. It was chosen for testing because it is very common and extremely cheap, while still providing excellent flexural and damping properties. A sample of butyl rubber having a rectangular cross section was loaded

into the cyclic loading machine and loaded at 1, 5, 10, 15 and 18.52 Hz.. Storage modulus and loss factor data were found from the data generated by the cyclic loading machine. Table 6.2 shows the stiffness and loss factor data at the frequency listed above.

Table 6.2 Butyl material properties as a function a frequency.

frequency [Hz]	Storage modulus [MPa]	shear modulus [MPa]	Loss factor
1	5.5556	1.8896	0.1121
5	6.2841	2.1374	0.1429
10	6.6737	2.2699	0.1841
15	7.6246	2.5934	0.2415
18.52	8.3378	2.8359	0.3512

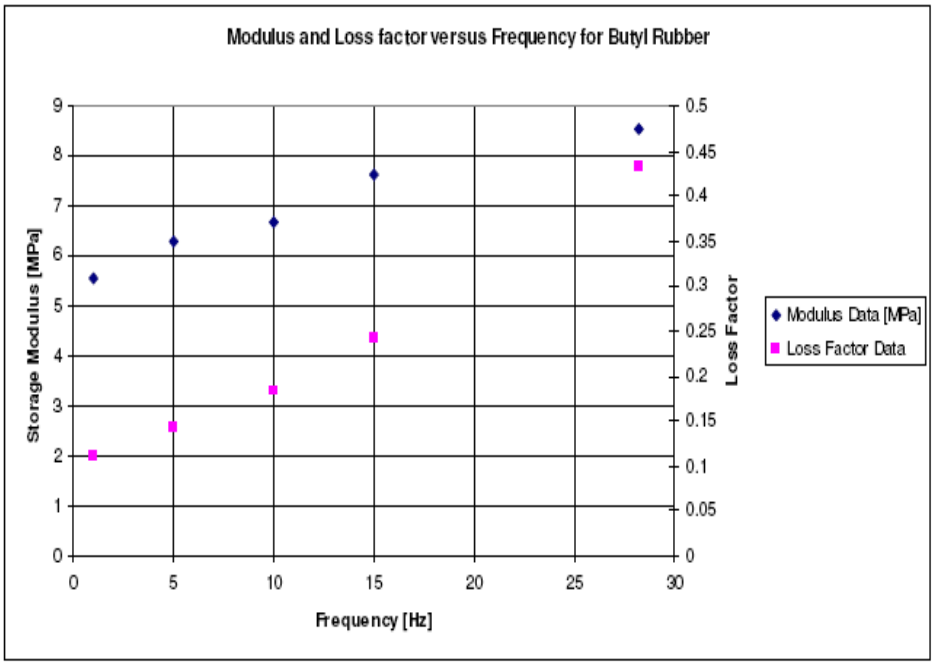

Fig 6.2 shows the trends of loss factor and storage modulus with frequency.

It is seen from Figure 6.2 that both the storage modulus and loss factor increase with increasing frequency. Over this relatively small frequency range, the loss factor almost quadruples its value as the frequency is increased from 1 Hz to 18.52 Hz. The storage odulus of the sample also sees fairly significant increases from 5.55 MPa to 8.55 MPa, about 1.5 times the original value at 1 Hz. Based on the low frequency and moderate temperature (the materials were tested at room temperature of about 70 degrees), the material is most likely operating in its rubbery region. Butyl rubber typically has a service temperature range of about -13 – 248 degrees Fahrenheit. At higher frequency it should be expected that the loss factor will continue to rise along with the storage modulus into the transition region.

6.2 Silicone 50A Rubber Testing

A sample of silicone 50A rubber was also tested using the cyclic loading machine. This sample of silicone rubber had a slightly higher durometer of 50A and exhibits greatly increased damping when compared to the silicone 30A sample. Table 6.3 gives the storage modulus and damping value for silicone 50A at 1, 5, 10, 15, and 18.52 Hz.

Table 6.3 Silicon Rubber material properties as a function a frequency

frequency [Hz]	Storage modulus [MPa]	shear modulus [MPa]	Loss factor
1	2.8811	0.9799	0.0263
5	2.7351	0.9303	0.0347
10	2.468	0.8394	0.0437
15	1.6567	0.5635	0.1054
18.52	1.824	0.6204	0.2115

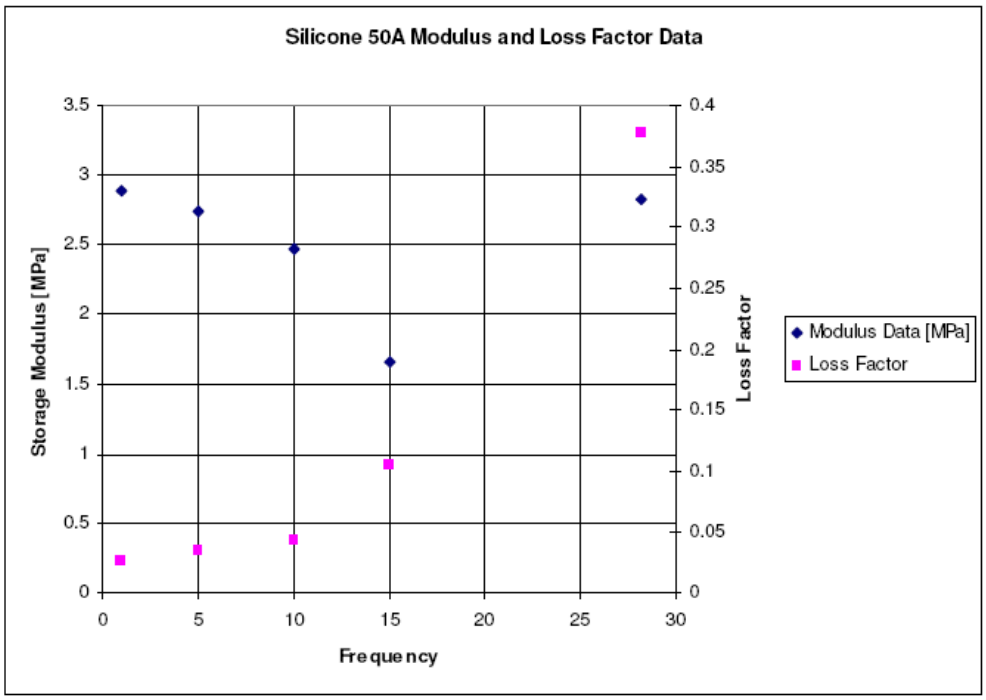

Fig 6.3Storage Modulus and loss factor data for silicone 50A rubber.

Figure 6.3 shows a steady decrease in storage modulus with increasing frequency from 1 to 15 Hz. However, the storage modulus spikes at or around 18.52 Hz. The loss factor shows a steady increase with increasing frequency. This suggests that the material has not yet entered the transition region.

Chapter 7

EXPERIMENTATION

7.1 Experimental set-up and Description:-

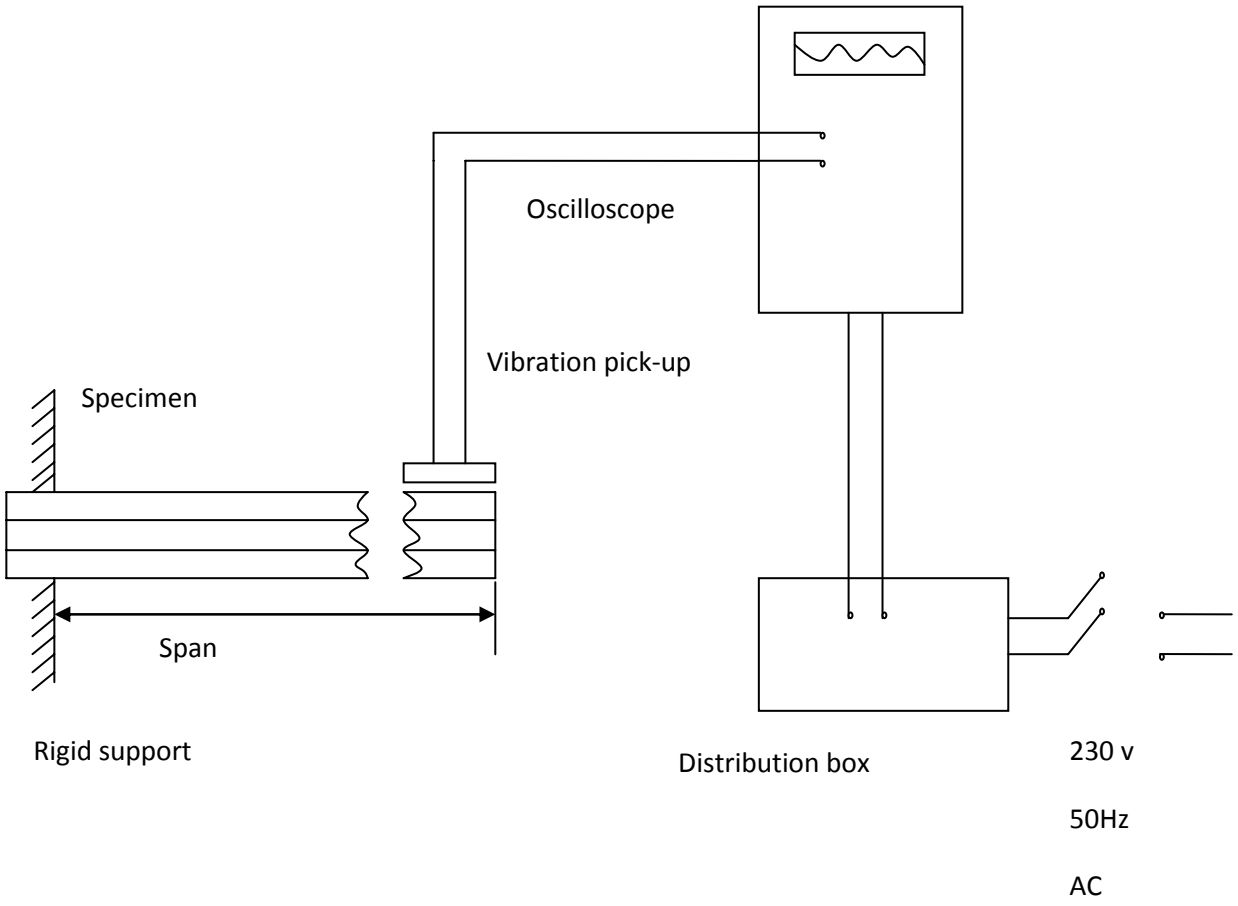

Fig 7.1: Schematic diagram of experimental setup with sandwich beam configuration

Fig: 7.2 photograph of experimental setup at dynamics lab

Fig7.3: photograph of sandwich specimen with pvc core

Test Specimen

The test specimen was a typical sandwich beam made of three layers, consisting two elastic layers and one viscoelastic layer at core as shown in fig 7.3, and the configuration of the beam has been shown in fig 5.1. The details of the specimen are as follows:

Table 7.1 Test specimen details

Layer no.	Layer configuration	Type of Material	Cross-section(mm)
1	Lower layer	Mild steel	580x40x5
2	Middle layer	Polyvinylchloride (PVC)	580x40x1.5
3	Upper layer	Mild steel	580x40x1

Instrumentation: In order to measure the logarithmic damping decrement, natural frequency of vibration of different specimen the following instruments were used as shown in circuit diagram figure:-

(1) Power supply unit

(2) Vibration pick-up

(3) Load cell

(4) Oscilloscope

(5) Dial gauge

Load Cell Specifications

(1) Capacity :- 5 tones

(2) Safe Over load :- 150 % of rated capacity

(3) Maximum Overload:- 200 % of rated capacity

(4) Fatigue rating :- 105 full cycles

(5) Non-linearity:- ± 1% of rated capacity or better

(6) Hysteresis :- ± 0.5 % of rated capacity or better

(7) Repeatability :- ± 0.5 % of rated capacity or better

(8) Creep error :- ± 1% of rated capacity or better

(9) Excitation: - 5 volts D.C.

(10) Terminal Resistance:-350Ω (nominal)

(11) Electrical connection :- Two meters of six core shielded cable/connected

(12) Temperature:- ± 10ċ to 50 ċ

Manufacturer - Syscon instruments private limited, Bangalore

Environmental

(1) Safe operating temperature:- + 10ċ to + 50ċ

(2) Temperature range for which specimen hold good :- +20ċ to + 30ċ

Oscilloscope

Display: - 8x10 cm. rectangular mono-accelerator c.r.o. at 2KV e.h.t. Trace rotation by front panel present. Vertical Deflection: - Four identical input channels ch1, ch2,ch3,ch4.

Band-width:- (-3 db) d.c. to 20 MHz (2 Hz to 20 MHz on a.c.)

Sensitivity: - 2 mV/cm to 10 V/cm in 1-2-5 sequence.

Accuracy: - ± 3 %

Variable Sensitivity :-> 2.5 % 1 range allows continuous adjustment of sensitivity from 2mV/cm to V/cm.

Input impedance: - 1M/28 PF appx.

Input coupling: - D.C. and A.C.

Input protection: - 400 V d.c.

Display modes: - Single trace ch1 or ch2 or ch3 or ch4. Dual trace chopped or alternate modes automatically selected by the T.B. switch.

Fig7.4 Oscilloscope

An oscilloscope measures two things:

- Voltage
- Time (and with time, often, frequency)

An electron beam is swept across a phosphorescent screen horizontally (X direction) at a known rate (perhaps one sweep per millisecond). An input signal is used to change the position of the beam in the Y direction. The trace left behind can be used to measure the voltage of the input signal (off the Y axis) and the duration or frequency can be read off the X axis.
An oscilloscope is a test instrument which allows you to look at the 'shape' of electrical signals by displaying a graph of voltage against time on its screen. It is like a voltmeter with the valuable extra function of showing how the voltage varies with time. A graticule with a 1cm grid enables you to take measurements of voltage and time from the screen.

The graph, usually called the trace, is drawn by a beam of electrons striking the phosphor coating of the screen making it emit light, usually green or blue. This is similar to the way a television picture is produced.

Oscilloscopes contain a vacuum tube with a cathode (negative electrode) at one end to emit electrons and an anode (positive electrode) to accelerate them so they move rapidly down the tube to the screen. This arrangement is called an electron gun. The tube also contains electrodes to deflect the electron beam up/down and left/right. The electrons are called cathode rays because they are emitted by the cathode and this gives the oscilloscope its full name of cathode ray oscilloscope or CRO.

A **dual trace** oscilloscope can display two traces on the screen, allowing you to easily compare the input and output of an amplifier for example. It is well worth paying the modest extra cost to have this facility.

Measuring voltage and time period:

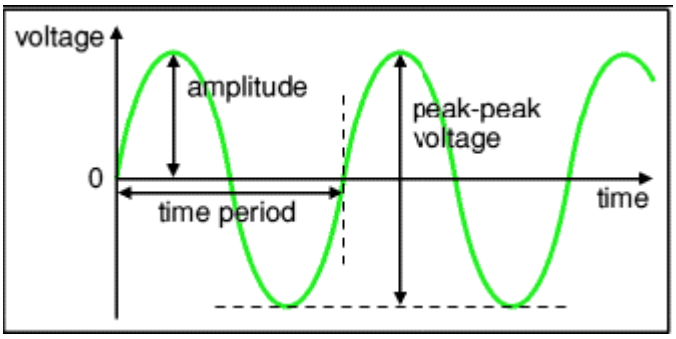

Fig.7.5 Relation between voltage and time

The trace on an oscilloscope screen is a graph of voltage against time. The shape of this graph is determined by the nature of the input signal.

In addition to the properties labeled on the graph, there is frequency which is the number of cycles per second. The diagram shows a sine wave but these properties apply to any signal with a constant shape.

- Amplitude is the maximum voltage reached by the signal. It is measured in volts, V.
- Peak voltage is another name for amplitude.
- Peak-peak voltage is twice the peak voltage (amplitude). When reading an oscilloscope trace it is usual to measure peak-peak voltage.
- Time period is the time taken for the signal to complete one cycle. It is measured in seconds (s), but time periods tend to be short so milliseconds (ms) and microseconds (μs) are often used. 1ms = 0.001s and 1μs = 0.000001s.

- Frequency is the number of cycles per second. It is measured in hertz (Hz), but frequencies tend to be high so kilohertz (kHz) and megahertz (MHz) are often used. 1kHz = 1000Hz and 1MHz = 1000000Hz.

Frequency = 1/time period and time period = 1/frequency

Dial Indicator: Dial indicator are instruments used to accurately measure a small distance. They may also be known as a dial gauge, Dial test indicator (DTI), or as a "clock". They are named so because the measurement results are displayed in a magnified way by means of a dial. Dial indicator may be used to check the variation in tolerance during the inspection process of a machined part, measure the deflection of a beam or ring under laboratory conditions, as well as many other situations where a small measurement needs to be registered or indicated.

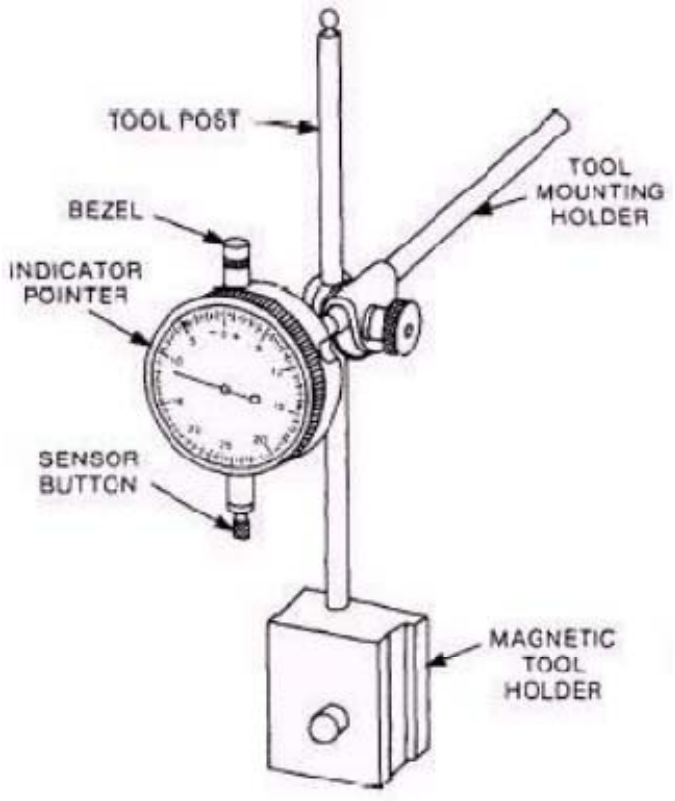

Fig7.6 Dial indicator

Vibration pick-up:- Type: - MV-2000. Specifications:-

(1) Dynamic frequency range :- 2 c/s to 1000 c/s

(2) Vibration amplitude: - ±1.5 mm max.

(3) Coil resistance :- 1000Ω

(4) Operating temperature :- 10ċ to 40 ċ

(5) Mounting :- by magnet

(6) Dimensions :- Cylindrical

Length:-45 mm

Diameter: - 19 mm

(7) Weight:- 150 gms

Fig7.7 vibration pick-up

Velocity Transducer: The velocity pickup is a very popular transducer or sensor for monitoring the vibration of rotating machinery. This type of vibration transducer installs easily on machines, and generally costs less than other sensors. For these two reasons, this type of transducer is ideal for general purpose machine applications. Velocity pickups have been used as vibration transducers on rotating machines for a very long time, and they are still utilized for a variety of applications today. Velocity pickups are available in many different physical configurations and output sensitivities.

Chapter 8

Results and Discussion

8.1. Experimental results

Loss factor measurement of the undamped and damped cantilever beam:

The test specimen was tested at dynamics lab of mechanical department as described in the experimentation chapter. The details of properties of undamped beam has already been described in section 6.1.The details of complex modulus properties of polyvinylchloride and properties of mild steel are as follows:

Table 8.1 properties of materials used in the test specimen [1, 2, 60]

Type of material	Elastic or storage Modulus E [MPa]	Density(ρ) [kg/m^3]	Loss factor (η)	Poison'ratio (υ)
Mild steel	210 x10^3	7860	----------	0.3
PVC	0.15	1700	0.4	0.46

8.1.1 Response of undamped beam

Before the addition of damping layers to the cantilever beam, the loss factor of the undamped beam was determined. The instrumentation outlined in section 6.0 was used to gather data for analysis using Microsoft Excel. Furthermore, once the data had been plotted for acceleration vs. time, the logarithmic decrement could be taken to determine damping factors (Meirovitch, 2001). These damping factors could then be used to find the loss factor. The logarithmic decrement is given by

$$\delta = \frac{1}{N}\ln\left(\frac{x_1}{x_2}\right) \qquad \text{---------- (8.1)}$$

Where N is the number of cycles between acceleration values 1 *x* and 2 *x*. The acceleration values are shown in the sample acceleration versus time plot in fig (8.1).

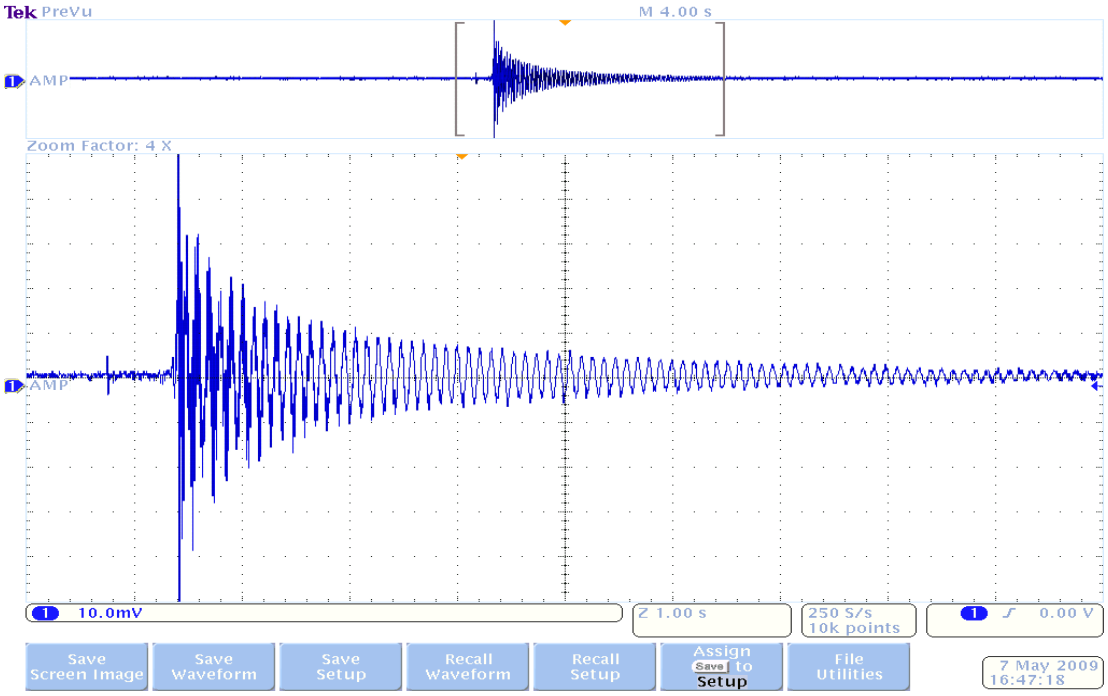

Fig 8.1(a) response of undamped beam (screen image)

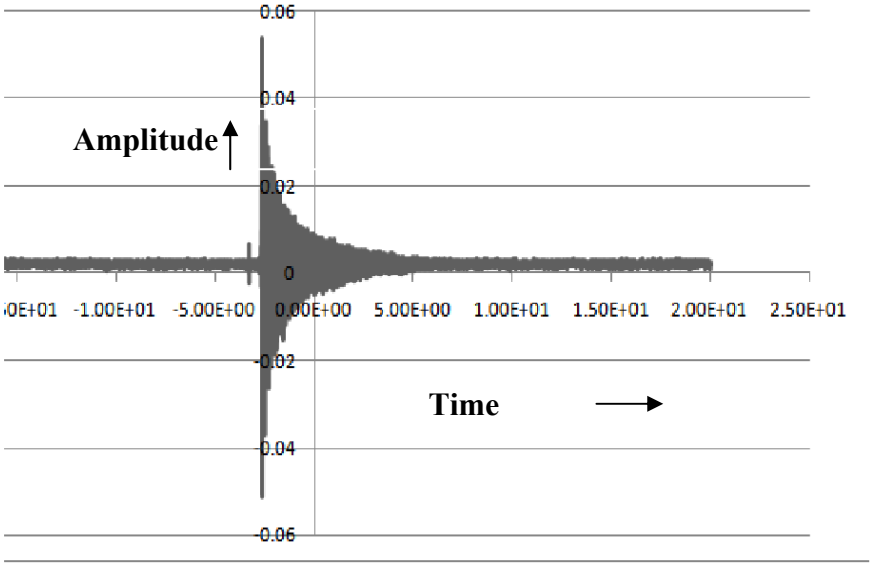

Fig 8.1(b) response of undamped beam (actual waveform data)

Once the logarithmic decrement was determined, the damping factor and loss factor were determined by

$$\xi = \frac{\delta}{\sqrt{4\pi^2 + \delta^2}}$$

$$\eta = 2\xi \qquad \text{---------- (8.2)}$$

This is a straight-forward and accurate method of determining the loss factor for the cantilever beam. It should be noted that the loss factor, η , is only two times the damping factor, ζ , at resonance frequencies.

Three tests were conducted on the undamped beam and the frequency of oscillation and loss factors determined for each test. The results are concluded in Table 8.2

Table 8.2 experimental frequency and loss factor data for undamped cantilever beam

Test no.	Acceleration point 1[mv]	Acceleration Point 2[mv]	Time 1 [s]	Time 2 [s]	Frequency [Hz]	Log decrement	Loss factor
1	33.2	23.4	-2.8	-2.38	24.2	0.0085	0.0027
2	8.6	6.4	-.280	.550	25.6	0.0035	0.0011
3	7.4	4.8	-.32	.66	24.7	0.0067	0.0021

The experimental data for time is coming like that (because reference point had not been set properly. From Table 8.2, it is seen that the average experimental vibrating frequency is 24.9 Hz. The calculated first modal frequency of the beam in section 6.1 was 18.52 Hz. There is a

difference of about 7.5% between the measured frequency and the first modal frequency of the beam. However, the beam, in actuality, does not vibrate at the first modal frequency, but rather, there are a combination of an infinite number of modes for a continuous system each having a different "weight" which, when combined using modal analysis, produce the actual frequency and dynamics of the beam.

8.1.2 Response of damped beam

In this section damped sandwich beam with viscoelastic (PVC) core has been tested. The acceleration values are shown in the sample acceleration versus time plot in fig (8.2).

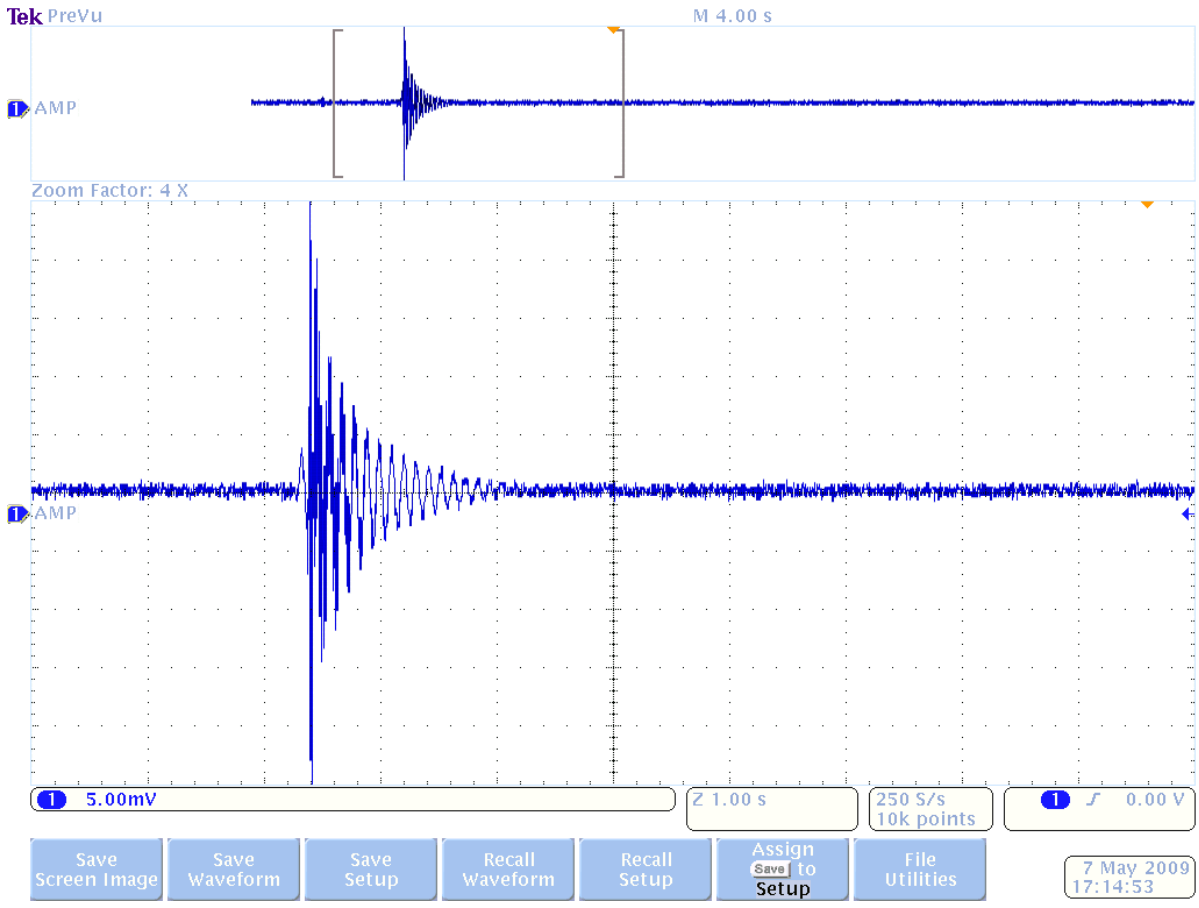

Fig 8.2(a) response of damped sandwich beam (screen image)

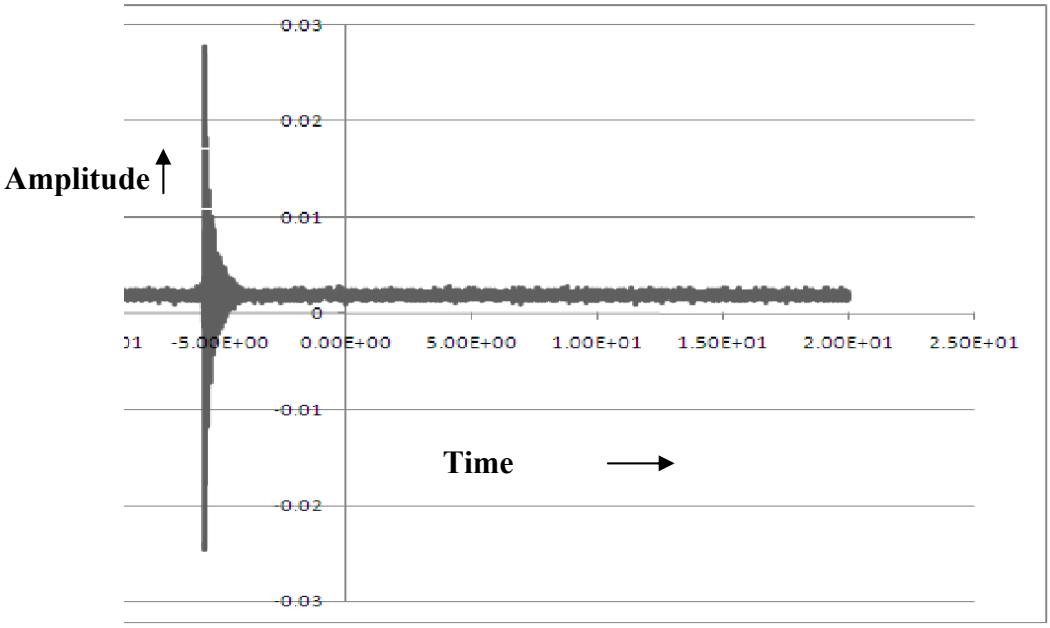

Fig 8.2(b) response of damped sandwich beam (actual wave form)

Three tests were conducted on the damped sandwich beam and the frequency of oscillation and loss factors determined for each test. The results are concluded in Table 8.3

Table 8.3 experimental frequency and loss factor data for undamped cantilever beam

Test no.	Acceleration point 1[mv]	Acceleration Point 2[mv]	Time 1 [s]	Time 2 [s]	Frequency [Hz]	Log decrement	Loss factor
1	9.8	6.3	-5.35	-5.0	18.6	0.0138	0.0043
2	5.9	4.4	-.6.5	-6.8	19.2	0.0154	0.0049
3	8.43	6.81	-6.35	-5.98	18.9	0.0113	0.0036

As we can see from the results shown above in the table 8.3 that the average experimental frequency is 18.9 Hz .The logarithmic decrement and loss factor has significantly increased for damped beam.

There is difference of 8.5% between the measured experimental frequency and the frequency obtained from the (finite element analysis) FEA of the damped sandwich beam with PVC core which will be discussed in the next section.

8.2 Results using Finite Element Analysis

The finite element analysis has been done using MATLAB program on the basis formulation shown in chapter 5. In this section FEA of the undamped beam and sandwich beam has been performed using the three different materials as viscoelastic core which are

1. Polyvinylchloride(PVC)
2. Butyl 50A rubber
3. Silicon 50A rubber

and the desired properties are given in the table 8.4.

Table 8.4 properties of the viscoelastic materials for modal analysis

Material type	Elastic modulus(E) [MPa]	Shear modulus(G) [MPa]	Density (ρ) [kg/m^3]	Loss factor(η)
PVC	150	51.36	1700	0.4
Butyle Rubber	8.3378	2.8359	1250	0.3512
Silicon Rubber	1.824	0.6204	1540	0.2115

8.2.1 Modal Analysis Results

For modal analysis of the beams geometric and mechanical properties of the specified materials is required, geometrical properties of the materials will be the same as shown in the table 7.1 and desired mechanical properties of the materials have been taken from the previous chapters are concluded in table 8.4.

The modal analysis results using MATLAB program for damped and undamped is concluded in the table 8.5-8.8.

Table 8.5 modal analysis of undamped beam

Mode no.	Modal frequency f_n (Hz)
1	18.616
2	116.67
3	326.75
4	640.47
5	1060.08

Table 8.6 modal analysis of sandwich beam with PVC core

Mode no.	Modal frequency f_n(Hz)	Modal Loss factor η_n
1	16.13	0.059
2	101.11	0.083
3	283.18	0.101
4	555.31	0.126
5	919.4	0.154

Table 8.7 modal analysis of sandwich beam with Butyl Rubber core

Mode no.	Modal frequency f_n(Hz)	Modal Loss factor η_n
1	12.411	0.035
2	77.77	0.084
3	217.83	0.139
4	427.16	0.192
5	707.23	0.243

Table 8.8 modal analysis of sandwich beam with Silicon Rubber core

Mode no.	Modal frequency f_n(Hz)	Modal Loss factor η_n
1	14.89	0.043
2	93.34	0.065
3	361.4	0.114
4	512.59	0.149
5	848.67	0. 216

It can be seen from table 8.6 to 8.8 that butyl rubber has the minimum value of natural frequency for the 1st mode and the percentage increase in loss factor is also more for increasing frequency as compared to pvc and silicon rubber. The amplitude for butyl rubber is also less compared to other two damping materials which has been shown below in harmonic analysis section. This indicates that butyl rubber has the better damping effect compared to other two damping materials.

However, it can be seen from table 8.6 and 8.8 that pvc has better damping effect than silicon rubber because the amplitude of pvc is less than silicon rubber (in harmonic analysis section) even though the value of natural frequency is greater for pvc.

8.2.2 Harmonic Analysis Results

In this section frequency response (harmonic) analysis has been performed using MATLAB program for specified beams, the response plots for beams with various materials is as follows:

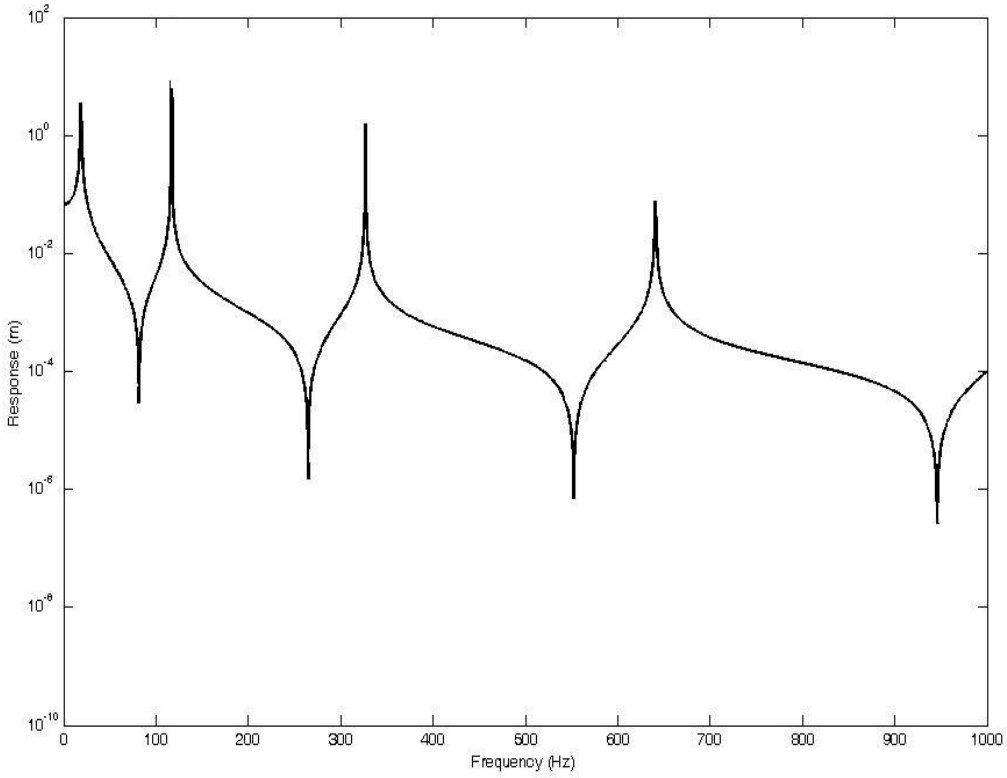

Fig 8.3 frequency response plot for undamped beam

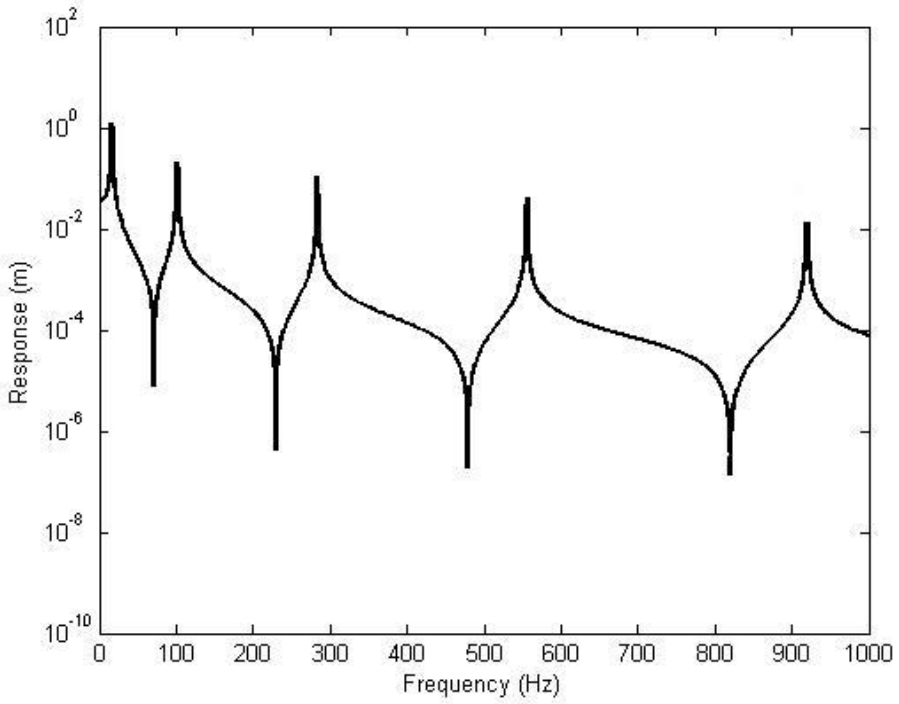

Fig 8.4 frequency response plots for damped beam with PVC core

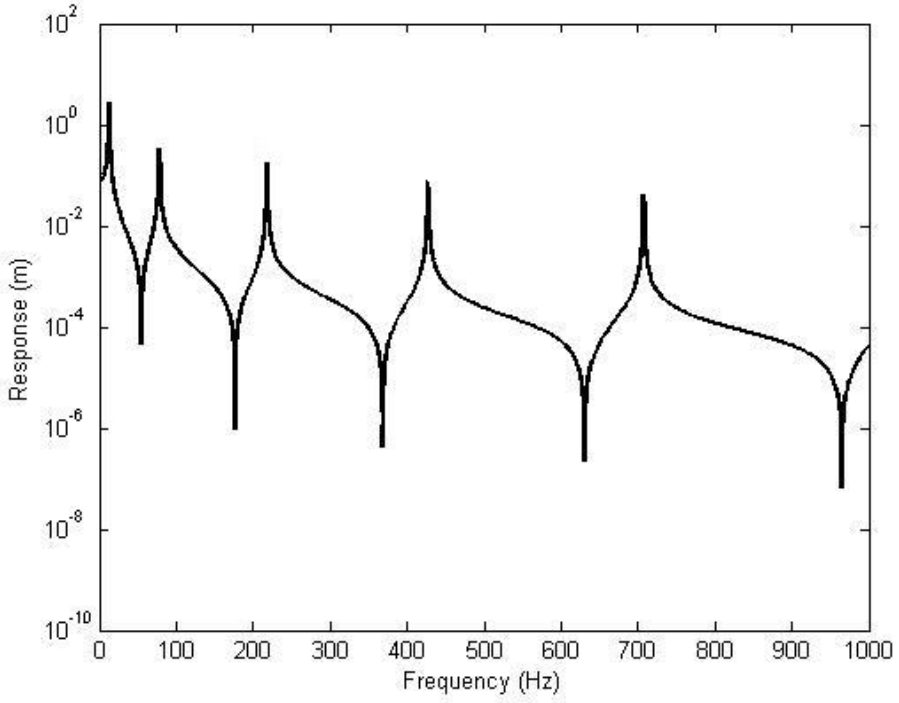

Fig 8.5 frequency response plots for damped beam with butyl Rubber core

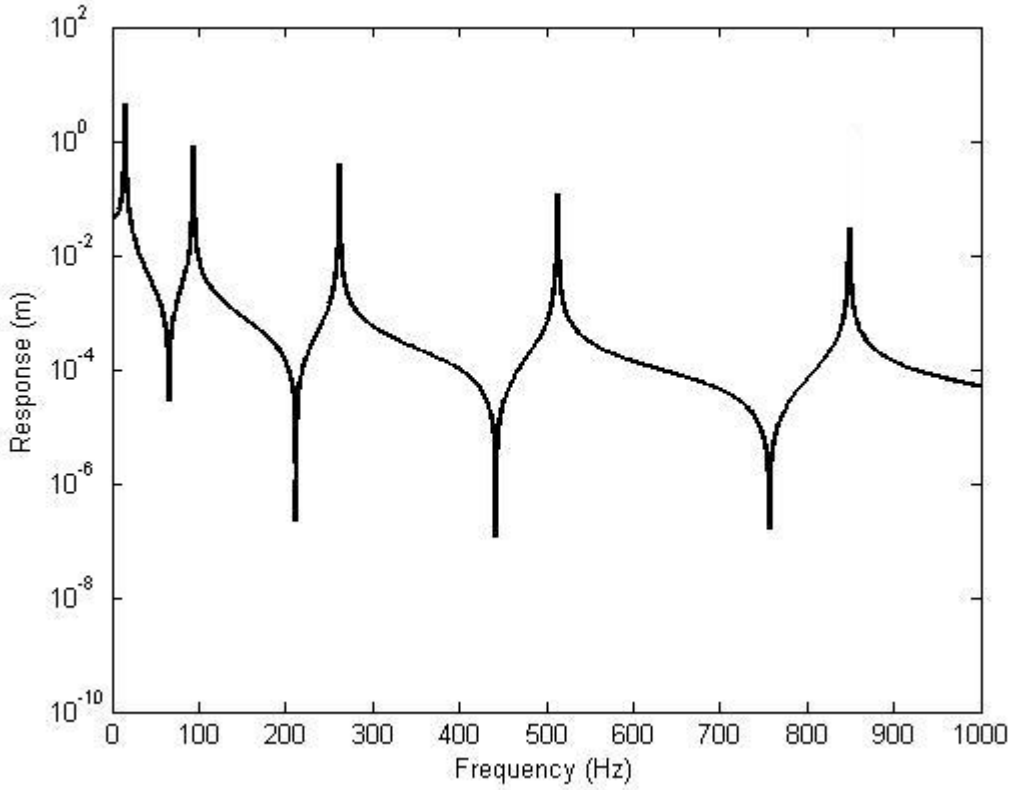

Fig 8.6 frequency response plots for damped beam with silicon Rubber core

In this section finite element analysis has been done by using two extra materials i.e. butyl rubber and silicon rubber along with PVC for the comparison of frequency responses.

It can be seen from tables of modal analyses (8.5-8.8) that the natural frequency for 1st mode for undamped beam is 18.616 which is very much near to frequency calculated theoretically which is 18.52 and finally the frequencies for the 1st mode for damped beam are 16.13, 12.411 and 14.89 for pvc, butyl rubber and silicon rubber respectively which are less than that of the undamped beam. Which shows that this damping technology significantly reduces the natural frequency of vibration of the system and response graphs (fig 8.3 – 8.7) for damped shows the amplitudes for each mode are also decreasing compared to undamped beam, which indicates that this method of damping treatment has a great significance in damping of structures. The results are finally superimposed into one graph (fig.8.7) which explains the results clearly.

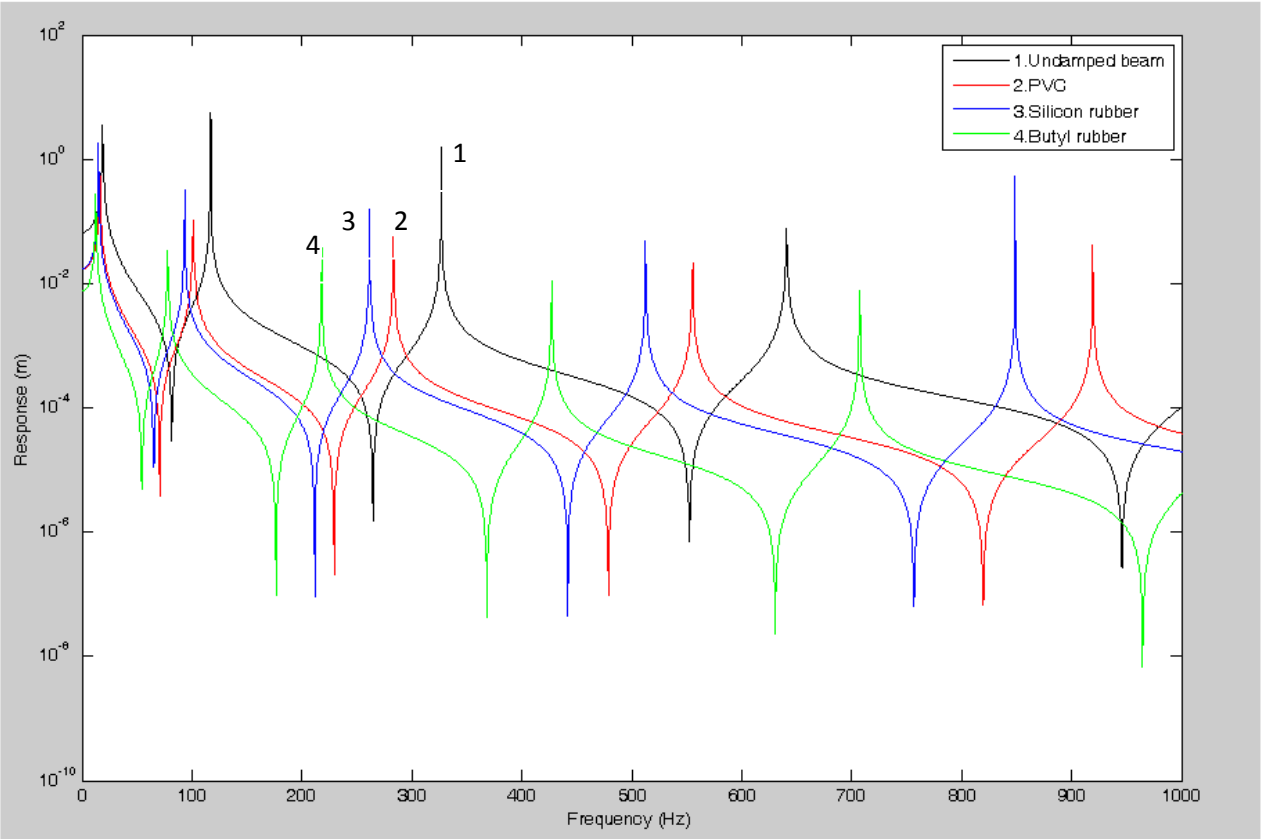

Fig 8.7 superimposed response

Chapter 9

Conclusion

The purpose of this report is to throw light on constrained layer viscoelastic damping, and trend for its application and to show the response by applying the theory of passive damping in a practical way, as well as with use of finite element analysis.

In this report damping treatment has been applied to cantilever beam and time response has been shown experimentally. This work has also been extended to finite element analysis of damped structure to show the frequency responses (harmonic response).

Results show that passive viscoelastic constrained layer damping treatment has a great significance in controlling the vibration of structures like beams, plates, etc. Perhaps the experimental data may not be absolutely accurate because of the environmental condition but this report can help in solving the vibration problem occurring in many mechanical systems according to the design requirements for different types of application.

Scope for Future Work

The conclusion found in the report this theory of damping treatment could be applied in structures concerned to vibration problem. One can use this theory to solve vibration problem by testing suitable damping material for structures according to the design requirements.

A different class of viscoelastic materials can be used for this purpose in future like viscoelastic foams (honeycomb structure) and materials with negative poison's ratio. From reference to some scientific articles [59] and journals its has been found that materials with negative poison's ratio have good capabilities in controlling the vibration and can be used for extreme damping, but the matter of concern is that the behavior of that materials must be studied properly by the designer.

References

1. Clarence W. de, Silva, *Vibration: Fundamentals and Practice*, Boca Raton, FL: CRC Press, cop. [2000].
2. Jones, D. I. G. 2001. *Handbook of Viscoelastic Vibration Damping.* West Sussex, England: John Wiley and Sons, LTD.
3. Nashif A.D., Jones D.I.G. and Henderson J.P., *Vibration Damping* ,Wiley, New York,1985.
4. Singiresu S.Rao., *The finite element method in engineering* ,Heinemann-Butterworth 2004.
5. Ross, D., Ungar, E., and Kerwin, E., 1959, "Damping of Flexural Vibrations by Means of Viscoelastic Laminate," *Structural Damping*, ASME, New York.
6. Kerwin, E.M. 1959. Damping of flexural waves by a constrained viscoelastic layer. Journal of the Acoustical Society of America, 31(7), 952-962.
7. DiTaranto, R. A., 1965, "Theory of Vibratory Bending for Elastic and Viscoelastic Layered Finite Length Beams," ASME J. Appl. Mech., **87**, pp. 881–886.
8. Mead, D.J., and Markus, S. 1969. The forced vibration of a three-layer, damped sandwich beam with arbitrary boundary conditions. Journal of Sound and Vibration. 10(2), 163-175.
9. Mead, D. J., 1970, "Loss Factors and Resonant Frequencies of Encastre Damped Sandwich Beams," J Sound Vib., **12**(1), pp. 99–112.
10. Rao, D. K., 1978, "Frequency and Loss Factors of Sandwich Beams under Various Boundary Conditions," J. Mech. Eng. Sci., **20(**5), pp. 271–282.
11. Yan, M.J., and Dowell, E.H. 1972. Governing equations for vibrating constrained-layer damping of sandwich beams and plates. Transactions of the ASME, Journal of Applied Mechanics, 94, 1041-1047.
12. Mead, D. J., 1982, "A Comparison of Some Equations for the Flexural Vibration of Damped Sandwich Beams," J. Sound Vib., **83**(3), pp. 363–377.
13. Yu, Y. Y., 1962, "Damping of Flexural Vibrations of Sandwich Plates," J. Aerosp. Sci., **29**, pp. 790–803.

14. Rao, Y. V. K. S., 1973, "Theory of Vibratory Bending of Unsymmetrical Sandwich Plates," Arch. Mech., **25**(2), pp. 213–225.
15. Sadasiva Rao, Y. V. K., and Nakra, B. C., 1974, "Vibrations of Unsymmetrical Sandwich Beams and Plates With Viscoelastic Cores," J. Sound Vib., **34**(3), pp. 309–326.
16. Durocher, L. L., and Solecki, R., 1976, "Harmonic Vibrations of Isotropic Elastic, and Elastic Viscoelastic Three-Layered Plates," J. Acoust. Soc. Am., **60(**1), pp. 105–112.
17. Kung, S. W., and Singh, R., 1998, "Vibration Analysis of BeamsWith Multiple Constrained Layer Damping Patches," J. Sound Vib., **212**(5), pp. 781–805.
18. Lall, A. K., Asnani, N. T., and Nakra, B. C., 1988, "Damping Analysis of Partially Covered Sandwich Beams," J. Sound Vib., **123 (**2), pp. 247–259.
19. Ghinet, S., 2005, "Statistical Energy Analysis of the Transmission Loss of Sandwich and Laminate Composite Structures," Ph.D. thesis, Department of Mechanical Engineering, Sherbrooke University, Québec, Canada.
20. Jones D.I.G. 1986, Journal of Sound and Vibration 106 353-356. The impulse response function of a damped single degree of freedom system
21. Huang T. C. and Huang C. C. 1971 Journal of Applied Mechanics 38, 515-521. Free vibrations of viscoelastic Timoshenko beams.
22. Cochardt A. W 1954 Journal of Applied Mechanics 22,257-262. A method for determining the internal damping of machine members.
23. Lemerle, P. 2002. Measurement of the Viscoelastic Properties of Damping Materials: Adaptation of the Wave Propagation Method to Tests Samples of Short Length. Journal of Sound and Vibration. 250: 2:181-196.
24. Hao, M. and M. D. Rao. 2005. Vibration and Damping Analysis of a Sandwich Beam Containing a Viscoelastic Constraining Layer. Journal of Composite Materials. 39: 18:1621-1643.
25. Lakes R. S. Viscoelastic measurement techniques ,2004 American institute of physics .Department of Engineering Physics, Engineering Mechanics Program, University of Wisconsin-Madison,147 Engineering Research Building, 1500 Engineering Drive, Madison, Wisconsin 53706-1687.

26. Sainsbury*M.G., Zhang Q.J. The Galerkin element method applied to the vibration of damped sandwich beams. Computers and Structures ,71 (1999) 239-256
27. Johnson CD, et al. Finite element prediction of damping in structures with constrained viscoelastic layers. AIAA Journal 1982; 20(9):1284-90.
28. Johnson CD, et al. Finite element prediction of damping in beams with constrained viscoelastic layers. Shock and Vibration Bulletin 1981; 51(1):71-81.
29. Soni ML. Finite element analysis of viscoelastically damped sandwich structures. Shock and Vibration Bull 1981; 55(1):97-109.
30. Ahmed KM. Free vibration of curved sandwich beams by the method of finite elements. Journal of Sound and Vibration 1971; 18(1):61-74.
31. Sainsbury MG, Ewins DJ. Vibration analysis of a damped machinery foundation structure using the dynamic sti€ness coupling technique. Journal of Engineering for Industry, Transactions of ASME 1974; 96(3):1000-1005.
32. Bisco AS, Springer GS. Analysis of free damped vibration of laminated composite plates and shells. International Journal of Solids and Structures 1989; 25:129-49.
33. Nakra B. C.,vibration controls in machines and structures using viscoelastic damping, Journal of Sound and Vibration (1998),211(3)449-465.
34. Myklestad N. O. 1952 Journal of Applied Mechanics 19, 284-286. The concept of complex damping.
35. Corsarov R.D. Sperling L.H. , Sound and Vibration Damping with Polymers, ACS Symposium Series, Vol. 424, American Chemical Society, Washington, DC, 1990.
36. Madigosky W.M., Lee G.F., Improved resonance technique for materials characterization, Journal of the Acoustical Society of America 73 (1983) 1374–1377.
37. Rogers L.Operators and fractional derivatives for viscoelastic constitutive equations, Journal of Rheology 27 (1983) 351–372.
38. Capps R.N., Dynamic Young's moduli of some commercially available polyurethanes, Journal of the Acoustical Society of America 73 (1983) 2000–2005.
39. Fowler, B.L. Interactive characterization and data base storage of complex modulus data, Proceedings of Damping'89, West Palm Beach, FL, Vol. 2, FAA 1-12, 1989.
40. . Nashif, A.D Lewis, T.M. Data base of dynamic properties of materials, Proceedings of Damping '91, San Diego, CA, Vol. 1, DBB 1-26, 1991.

41. Jones D.I.G., Results of a Round Robin test program: complex modulus properties of a polymeric damping material, WL-TR-92-3104, Technical Report, Wright Laboratory, Dayton, Ohio, 1992.
42. Caputo, M. Mainardi,F. A new dissipation model based on memory mechanism, Pure and Applied Geophysics 91 (1971) 134–147.
43. Bagley R.L., Torvik P.J., Fractional calculus-a different approach to the analysis of viscoelastically damped structures, American Institute of Aeronautics and Astronautics Journal 2 (1983) 741–748.
44. Bagley R.L., Torvik P.J. On the fractional calculus model of viscoelastic behavior, Journal of Rheology 30 (1986) 133–135.
45. Koh, C.G. Kelly J.M., Application of fractional derivatives to seismic analysis of base-isolated models, Earthquake Engineering and Structural Dynamics 19 (1990) 229–241.
46. Makris, N. Constantinou, M.C. Fractional derivative Maxwell model for viscous damper, Journal of Structural Engineering, American Society of Civil Engineers 117 (1991) 2708–2724.
47. Friedrich,C. Braun,H. Generalized Cole–Cole behaviour and its rheological relevance, Rheologica Acta 31 (1992) 309–322.
48. Mainardi, F. Fractional relaxation in anelastic solids, Journal of Alloys and Compounds 211/212 (1994) 534–538.
49. Enelund,M. Olsson P., Damping described by fading memory models, Proceedings of the 36th AIAA/ASME/ ASCE/AHS Structures, Structural Dynamics and Materials Conference, New Orleans, LA, 1995, Vol. 1 pp. 207–220.
50. Fenander,A. Modal synthesis when modeling damping by use of fractional derivatives, American Institute of Aeronautics and Astronautics Journal 34 (1996) 1051–1058.
51. Pritz, T. Analysis of four-parameter fractional derivative model of real solid materials, Journal of Sound and Vibration 195 (1996) 103–115.
52. Shimizu,N. Zhang,W. Fractional calculus approach to dynamic problems of viscoelastic materials, JSME International Journal, Series C 42 (1999) 825–837.

53. Ouis D., Characterization of rubber by means of a modified Zener model, Proceedings on CD-ROM of the International Rubber Conference, Birmingham, 2001, pp. 559–570.
54. Pritz, T. On the behaviour of fractional derivative Maxwell model, Computational Acoustics, Proceedings on CD-ROM of the 17th International Congress on Acoustics, Rome, Vol. 2, 2001, pp. 32–33.
55. Havriliak, S. Negami S., A complex plane representation of dielectric and mechanical relaxation processes in some polymers, Polymer 8 (1967) 161–210.
56. Lee G.F., Lee J.D., B. Hartmann, D. Rathnamma, Damping properties of PTMG/PPG blends, Proceedings of Damping'93, San Francisco, Vol. 3, ICA 1-19, 1993.
57. Gallimore Craig A. "Passive Viscoelastic Constrained Layer Damping Application for a small Aircraft Landing Gear System" master's thesis 2008, Virginia Polytechnic Institute and State University, Blacksburg, VA
58. Meirovitch L. 1975, *Elements of Vibration Analysis,* McGraw hill publication.
59. http://home.um.edu.mt/auxetic/properties.htm
60. James Mark, *Physical Properties of Polymers Handbook* **,** Springer**, 2007**

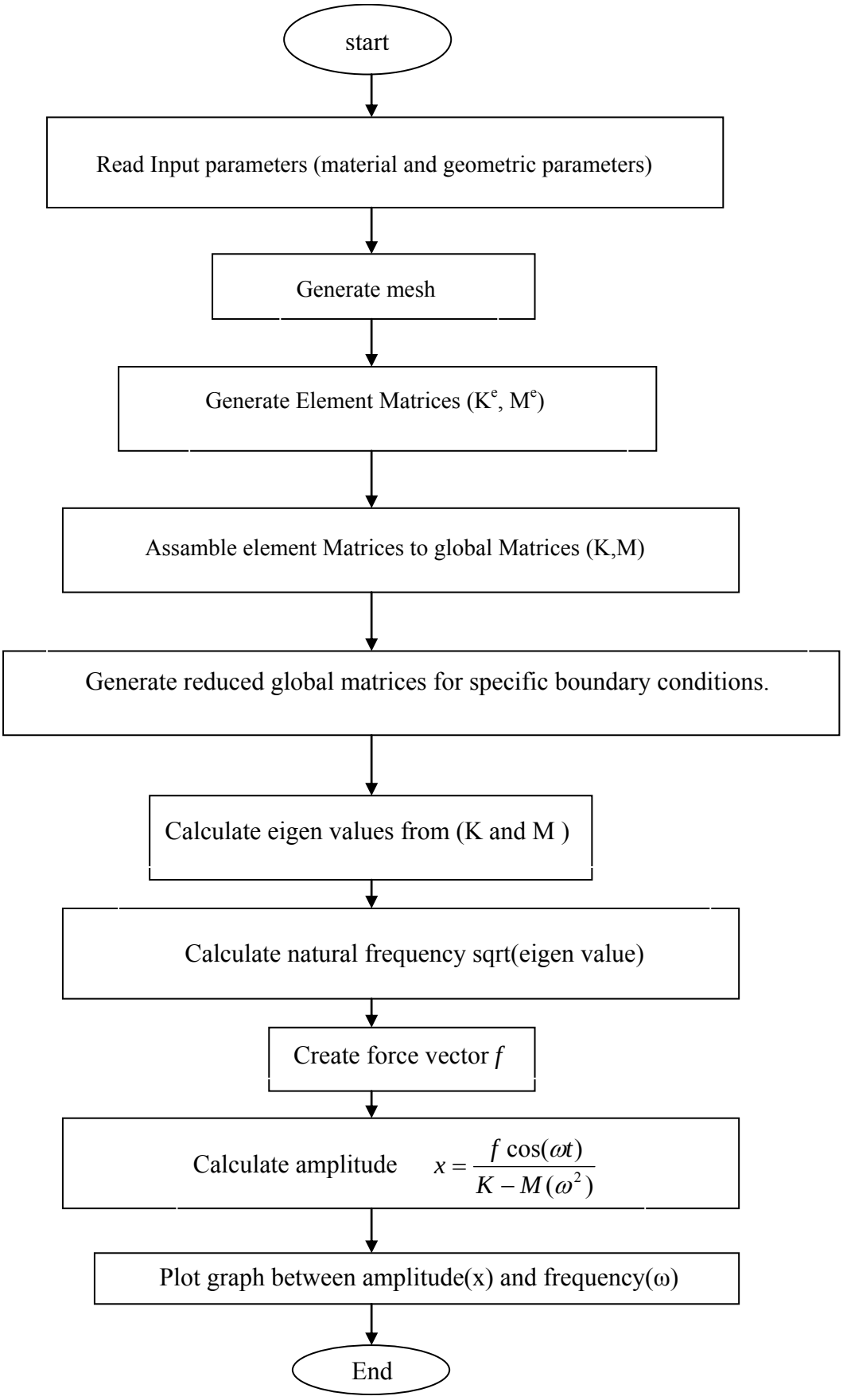

Flow chart for MATLAB program